Genomic engineering at the Roco4 & mybW locus in Dictyostelium discoideum using CRISPR/Cas9

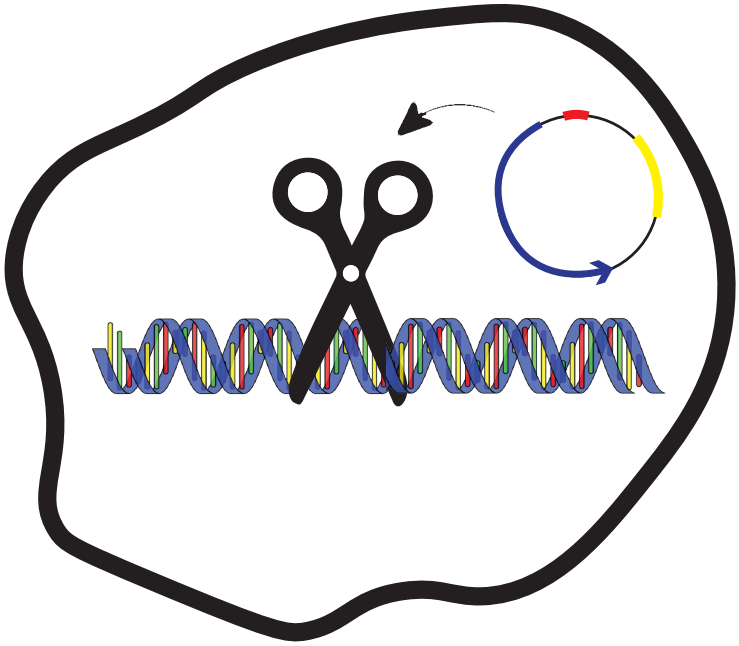

Wyco Zweekhorst
Dr. Eelco Tromer
Gargi Ahuja
Dr. Arjan Kortholt
S5432928
13-05-2024

rijksuniversiteit groningen

Abstract

Dictyostelium is an important eukaryotic model organism for research into basic cell biological mechanisms. It can be used to study systems such as growth, micropinocytosis, cell mortality, chemotaxis, and signal transduction during development. Recently, CRISPR/Cas9 has been added to the toolbox for functional analysis in Dictyostelium, which makes it possible to modify genomes at a higher efficiency. The aim of this project was to implement the CRISPR/Cas9 system for Dictyostelium in the cell biochemistry lab using Roco4 and mybW as the model genes. To achieve this goal, Roco4 and mybW knockouts and GFP-inserts were generated using the CRISPR/Cas9 system. Post development of the knockouts and GFP-inserts, the *Roco4* knockouts and GFP-inserts served to give insight into the Role of Roco4 during phagocytosis. The main questions addressed whether it was possible to visualize Rab protein phosphorylation by Roco4 during phagocytosis and if Roco4 plays a role in phagosomal uptake and maturation. In the end, no successful CRISPR/Cas9 knockouts or GFP-inserts were generated for either *Roco4* or *mybW*. Consequently, the assays required to answer the questions surrounding the role of Roco4 in phagocytosis were performed using a pre-existing *Roco4 null* cell line. Through the use of an immunofluorescence assay utilizing the pT72-Rab8a antibody, this project successfully visualized the phosphorylation of Rab proteins by Roco4 in Dictyostelium cells. Additionally, this project showed that Roco4 is involved in the uptake process during phagocytosis and plays a role in phagosome maturation.

Table of Contents

Introduction

The social amoeba *Dictyostelium discoideum* has been used as an eukaryotic model organism to study basic cell biological mechanisms for several decades. (Iriki, et al., 2019) It has been used to study systems such as growth, micropinocytosis, cell mortality, chemotaxis, and signal transduction during development. (Sekine, et al., 2018) *D. discoideum* possesses homologues of genes in complex eukaryotes related to these processes. Some of these homologues are absent in the well-established model organism *Saccharomyces cerevisiae*, thus establishing *D. discoideum* as a crucial model organism for the investigation of those specific genes. (Eichinger, et al., 2005) On top of that, *D.discoideum* lacks the complexity of other model organisms such as the *Caenorhabditis elegans* and *Drosophila melanogaster*. (Yamashita, et al., 2021) Making it a popular model organism to study fundamental biological processes related to human diseases.

D.discoideum (Dictyostelium) is haploid, making it easy to generate genetic mutants and identify phenotypes without further manipulation. (Yamashita, et al., 2021) There is a wide range of genetic techniques available for Dictyostelium, including homologous recombination-based methods to create knockouts, knock-ins and point mutations. On top of that, it is possible to use expression vectors to study protein overexpression and expression of fusion-tagged proteins in Dictyostelium. (Gaudet, et al., 2007) (Veltman, et al., 2009) However, gene knockout methods based on homologous recombination are sometimes inefficient and time-consuming, especially for generating multiple gene knockouts. (Linkner, et al., 2012)

CRISPR/Cas9 has recently been added to the toolbox for functional analysis in Dictyostelium and makes it possible to modify genomes with a higher efficiency. CRISPR was developed from a prokaryotic adaptive immune system. (Muramoto, et al., 2019) It requires two components: a Cas9 nuclease with a nuclear localization signal (NLS) and a chimeric single-guide RNA (sgRNA). In the Dictyostelium CRISPR/Cas9 system, the Cas9 and sgRNAs are simultaneously expressed from an all-in-one vector. The Cas9/sgRNA complex recognizes a specific 20-nucleotide site alongside a protospacer adjacent motif (PAM) sequence. (Iriki, et al., 2019) Approximately 3 base pairs upstream of the PAM sequence the Cas9/sgRNA complex will induce a double-strand break (DSB) which is then repaired by non-homologous end joining (NHEJ) or homology directed repair (HDR). (Jinek, et al., 2012) NHEJ leaves insertions or deletions at the cleavage site, while the HDR pathway can introduce sequences encoding a fluorescent protein, tag, or point mutation into the gene of interest. (Chu, et al., 2015) (Lin, et al., 2014)In the type-II CRISPR/Cas9 system, which is wildly used, Cas9 nuclease, derived from *Streptococcus pyogenes* (SpCas9), recognizes a 5'-NGG-3' PAM sequence. (Muramoto, et al., 2019)

The PAM sequence is one of the primary considerations when designing guide RNA's. Since NGG appears at a relatively lower frequency within the AT-rich Dictyostelium genome this can limit the possibilities of creating knockouts and especially knock-ins. (Muramoto, et al., 2019) Furthermore, the minimalization of off-target effects is another important consideration. Off-targets trigger unintended

mutations within the genome. To minimize off-target effects, the target sequence must be unique compared to the rest of the genome.

The aim of this project was to implement the CRISPR/Cas9 system for Dictyostelium in the cell biochemistry lab using *Roco4* and *mybW* as the model genes, ultimately leading to the creation of knockouts and GFP-inserts for both genes. The Dictyostelium Roco4 protein is a homologue of the Leucine-rich repeat kinase 2 (LRRK2) (Gilsbach et al., 2012), which shares the same domain architecture as LRRK2. (Kortholt, et al., 2012) LRRK2 is a commonly mutated gene in both sporadic and inherited forms of Parkinson's Disease (PD). (Jeong & Lee, 2020) In PD, LRRK2 kinase activity is often increased, which sequentially has many downstream effects, including impaired dopamine neurotransmission, dopaminergic neuronal cell death, protein synthesis and degradation defects, increased inflammatory response, and oxidative damage (Liou, et al., 2008); (Carballo-Carbajal, et al., 2010) (Chen, et al., 2012); (Maekawa, et al., 2016); (Rui, et al., 2018)

LRRK2 is a member of the Roco protein family, having Roc (Ras of complex) and COR (C-terminus of Roc) domains, along with a leucine-rich repeat (LRR) at its N-terminus (Rui, et al., 2018) It is a cytoplasmic protein that associates with intracellular membranes, such as the endoplasmic reticulum, and vesicular structures (Hatano, et al., 2007) (Alegre-Abarrategui, et al., 2009) and is highly expressed in dopaminergic neurons of the mammalian brain (Biskup, et al., 2006) (Galter, et al., 2006) (Higashi, et al., 2007). The structural and functional similarities of Roco4 and LRRK2, make Dictyostelium a very suitable model organism for studying LRRK2, since purification of LRRK2 or any fragments of it is a challenging task . (Gilsbach, 2014)

mybW is a homolog of the human Kinetochore-associated protein (KNL2). In humans, KNL2 and two other proteins, mis18α and mis18β, form a complex that localizes transiently to centromeres during a brief period of the cell cycle. This starts in the telophase and persists through early G1 phase. (Cheeseman & Desai, 2008) Creating CRISPR Knockouts and GFP-inserts of the *mybW* gene could give further insight into the functionality of *mybW* and its homolog.

Post development of the knockouts and GFP-inserts, the *Roco4* knockouts and GFP-inserts would serve to give insight into the Role of Roco4 during phagocytosis. The main questions being whether it is possible to visualize Rab protein phosphorylation by Roco4 during phagocytosis and if Roco4 plays a role in phagosomal uptake and maturation. The hypothesis was that Roco4 would phosphorylate Rab proteins as reported by a previous study (Rosenbusch, et al., 2021) and that it would be possible to visualize this process via an immunofluorescence assay utilizing the pt72 Rab8a antibody. On top of that it was expected that Roco4 would be an important factor in stimulating phagosome maturation since its homologue LRRK2 has been reported to recruit Rab proteins to phagosomes such as Rab8a and Rab7L1, which are known to play an important role in phagosome maturation. (Kuwahara et al., 2016; Steger et al., 2016a)

In order to reach these goals, Dictyostelium Roco4 and mybW knockouts and GFP-inserts were generated using the CRISPR/CAS9 system. The Roco4 transformants were then used in both an immunofluorescence and flow cytometry assay to investigate the role of Roco4 in phagocytosis.

Material and Methods

Selection of Cas9 vector

The all-in-one vector ptm1285 (Tetsuya Muramoto, 2022) was used for the construction of the Roco4 and *mybW* CRISPR/Cas9 plasmids. The ptm1285 vector consists of four modules; spCas9, tRNA-sgRNA (BPil), Amp resistance cassette and a neomycin resistance cassette, which are all build into a pBluescript II backbone. The spCas9 nuclease is derived from *Streptococcus pyogenes* and recognizes a 5'-NGG-3' PAM sequence. (Muramoto, et al., 2019)

Design of guide RNA's

The genes of interest for this project were *Roco4* and *mybW*. Possible PAM sequences in the *Roco4* sequence were identified using CRISPOR (Concordet & Haeussler, 2018). Potential gRNA sequences had to pass the following criteria: GC content higher than 20%, no four thymidine repeats and an out of frame score of 66 or higher. No 3' PAM sequences close enough to the stop codon were identified for the *Roco4* gene. At the 5' end of the gene, three PAM sequences were identified. These were located at 55 base pairs, 56 base pairs and 60 base pairs from the start codon and will be referred to as *Roco4_55*, *Roco4_56* and *Roco4*_60.

Two complementary oligonucleotides were designed per PAM Sequence.
These oligonucleotides contained the 20 nucleotides upstream from the PAM Sequence and a 4 nucleotide overhang common to BpiI mediated golden gate cloning. The overhang consisted of 5'-AGCA-'3 at the end of the sense oligonucleotide and 5'-AAAC-'3 at the end of the antisense oligonucleotide. This can be seen in Figure 1.

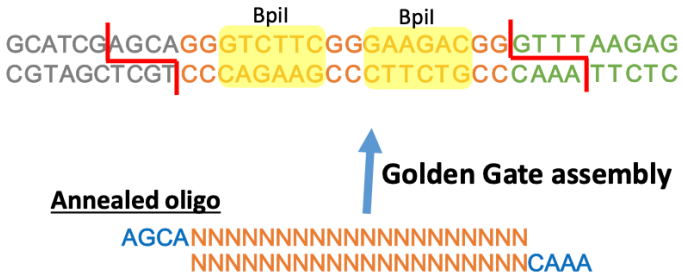

Figure 1 orientation of the gRNA's into the BpiI cut site *(Scientific Reports, 2018)*

The *mybW* target sequence, alongside its reverse complement, were taken from the following paper (Ogasawara et al., 2022). The 5'-AGCA-'3 was added at the end of the sense oligonucleotide and the 5'-AAAC-'3 at the end of the antisense oligonucleotide. The sequences of the final guide RNA's can be found in supplementary table 1.

Primer design for blast/GFP insertions

To use blasticidin resistance as a second selection marker for the knockouts, primers were designed to integrate a blast cassette at the 5' end of the target gene. Simultaneously primers were designed for the integration of GFP at the 5' end of the target gene. The primers for the blast and GFP insertions were designed to form homologous arms over the target gene and to integrate the blast or GFP gene at the 5' end. The homologous arms were designed to not include the start codon of the original gene to ensure proper translation and function of the insert. The primers for the *Roco4* GFP insertion consisted of 96 bp long homologous strands + 24 bp of the GFP sequence from the pdm1258 plasmid for amplification. The primers for the *mybW* GFP insertion consisted of 92 bp long homologous strands + 24 bp of the GFP sequence from the pdm1258 plasmid for amplification. The primers for the ROCO4 blast insertion consisted of 69 bp & 62 bp long homologous strands + 35 bp & 45 bp of the Blast sequence from the pdm326 plasmid for amplification. The primers for the *mybW* blast insertion consisted of 66 bp & 75 bp long homologous strands + 35 bp & 45 bp of the blast sequence from the pdm326 plasmid for amplification. The sequences of the blast and GFP primers can be found in supplementary table 1.

Molecular cloning of CRISPR/Cas9 constructs

To prepare for the golden gate reaction each of the sense and antisense oligos had to be annealed together. The annealing mixture consisted of 4.5 μL sense oligo (10 μM), 4.5 μL antisense oligo (10 μM), and 1 μL annealing buffer (10x) (400 mM Tris-HCl pH 8.0, 200 mM $MgCl_2$). The annealing was performed using a Bio-Rad® C1000 touch thermocycler under the following conditions: 95˚C for 5 min, followed by slowly cooling to 25˚C (-1˚ C/min).

Golden gate cloning

The initial golden gate reaction was set up under the following conditions: 4 μL ptm1285 (25 ng/μL), 2 μL T4 DNA ligase buffer (10x), 2 μL T4 DNA ligase (200 U/μL), 1.5 μL annealed oligo for target gene, 0.5 μL BbsI (20 U/μL) and 10 μL MilliQ. The reaction was then conducted under the following thermocycling conditions using a Bio-Rad® C1000 touch thermocycler: 37˚C for 5 minutes followed by 16˚C for 15 minutes, which was repeated 8 times. To ensure complete digestion and prevent contamination of the non-integrated vector an extra digestion step was performed. This digestion reaction was performed under the following conditions: 20 μL of golden gate reaction product, 2.5 μL 10x buffer G and 0.5 μL BbsI. This was incubated at 37˚C for 60 minutes followed by 80˚C for 5 minutes.

However, this initial set-up led to a large amount of background colonies after transformation into competent *E. coli*. During troubleshooting the amount of plasmid in the reaction was lowered, the digestion step was elongated and the concentration of BbsI was increased. None of these changes made a difference in the amount of background colonies. The next troubleshooting step was to use BpiI which is relatively the same enzyme as BbsI but from a different manufacturer. BpiI ended up making a big difference in the amount of background colonies and was used for the rest of the project.

The final golden gate reaction was set up under the following conditions: 4 μL ptm1285 (25 ng/μL), 2 μL T4 DNA ligase buffer (10x), 2 μL T4 DNA ligase (200 U/μL), 1.5 μL annealed oligo for target gene, 1 μL BPiI (10 U/μL) and 9.5 μL MilliQ. The reaction was then conducted under the following thermocycling conditions using a Bio-Rad® C1000 touch thermocycler: 37˚C for 5 minutes followed by 16˚C for 15 minutes, which was repeated 8 times. The extra digestion step was performed under the following conditions: 20 μL of golden gate reaction product, 2 μL 10x buffer G and 1 μL BpiI. The mixture was incubated at 37˚C for 60 minutes followed by 80˚C for 5 minutes.

Transformation

In order to transform chemically competent *E. coli*, 10 μL of the golden gate product was added to 50 μL of *E. coli* and put on ice for 15 minutes. This was followed by a heat shock at 42˚C for 1 minute and a recovery period on ice of 5 minutes. The complete 60 μL of *E. coli* was spread out on LB Agar plates containing ampicillin (50 μg/mL) and incubated at 37˚C overnight.

Colony PCR

To confirm successful cloning, a PCR was performed directly from 4-10 picked colonies from the LB Agar plates. The colonies were picked using a sterile pipette tip, then dissolved in 10 μL of MilliQ after which the pipette tips were inoculated in LB medium at 37˚C for DNA preparation. The milliQ solutions containing the colonies were heated to 95˚C for 5 minutes. After which, 2 μL of the solution was used as a template for the following PCR mixture: 2 μL (5x) HF Phusion buffer, 0.8 μL dNTPs (2.5 mM), 0.3 μL sense oligo for target (10 μM), 0.3 μL tracr-Rv-screen primer (10 μM), 0.125 μL Phusion® Polymerase (2000 U/mL) and 4.48 μL MilliQ. The primer sequence of tracr_Rv_screen can be found in supplementary table 2. The colony PCR was performed under the following conditions using a Bio-Rad® C1000 touch thermal cycler: an initial 98˚C for 30 seconds, followed by 30 cycles of 98˚C for 12 seconds, 60˚C for 30 seconds and 72˚C for 20 seconds which was followed by a final step of 72˚C for 10 minutes. The Prescence of PCR product was verified through gel electrophoresis using 1.5% agarose gels, where a band of 120 bp implied successful cloning.

DNA extraction & Sequencing

To prepare for transfection, the constructed plasmids had to be extracted out of the inoculated colonies by miniprep. The miniprep was performed using the Nucleospin® Plasmid EasyPure kit following manufacturers protocol (Machery-Nagel, 2023). The concentration and purity of the extracted plasmids was measured using an Eppendorf® D30 BioPhotometer. After miniprep the samples were send for sequencing at Eurofins® to verify successful cloning. Per plasmid two samples were sent for sequencing, one with the Neo_up_seq primer and one with the tracr_Rv_screen primer. The sequences of the Neo_up_seq primer and tracr_Rv_screen primer can be found in supplementary table 2.

Amplification of blast and GFP

To create blast and GFP insertions, The blast and GFP sequences had to be amplified out of other plasmids. The blast sequences for the *Roco*4 & *mybW* CRISPR/Cas9

plasmids were amplified from pdm326. The plasmid map of pdm326 can be found in supplementary figure 2. The PCR mixture for the blast insert that would pair with the *Roco4* CRISPR plasmids consisted of 1 μL HR5-ACT6-ROCO4 (25 μM), 1 μL HR3-mhcA-ROCO4 (25 μM), 1 μL pdm326 (25 ng/μL), 1 μL Phusion® Polymerase, 10 μL Phusion® HF buffer (5x), 4 μL dNTPs (2.5 mM) and 32 μL MilliQ.

The PCR mixture of the blast insert that would pair with the *mybW* CRISPR plasmids consisted of 1 μL HR5-ACT6-MybW (25 μM), 1 μL HR3-mhcA-MybW (25 μM), 1 μL pdm326 (25 ng/μL), 1 μL Phusion® Polymerase, 10 μL Phusion® HF buffer (5x), 4 μL dNTPs (2.5 mM) and 32 μL MilliQ. The sequences for HR5-ACT6-ROCO4, HR3-mhcA-ROCO4, HR5-ACT6-MybW and HR3-mhcA-MybW can be found in supplementary table 1.

The PCRs were performed under the following conditions using a Bio-Rad® C1000 touch thermal cycler: an initial 98˚C for 30 seconds, followed by 34 cycles of 98˚C for 10 seconds, 60˚C for 30 seconds and 72˚ C for 60 seconds which was followed by a final step of 72˚C for 10 minutes. The presence of PCR product was verified through gel electrophoresis using 1% agarose gels, where a band of 1500 bp implied successful amplification. The PCR product was then purified using the Nucleospin® Gel and PCR Clean-up kit following manufactures protocol. (Machery-nagel, 2023)

The GFP sequences for the *Roco*4 & *mybW* CRISPR/Cas9 plasmids were amplified from pdm1258. The plasmid map of pdm1258 can be found in supplementary figure 1.
The PCR mixture for the GFP insert that would pair with the *Roco4* CRISPR/Cas9 plasmids consisted of 1 μL HR5-GFP-ROCO (25 μM) 4, 1 μL HR3-GFP-ROCO4-new (25 μM), 1 μL pdm1258 (25 ng/μL), 1 μL Phusion® Polymerase, 10 μL (5x) Phusion® HF buffer, 4 μL dNTPs (2.5 mM) and 32 μL MilliQ.

The PCR mixture of the GFP insert that would pair with the *mybW* CRISPR/Cas9 plasmids consisted of 1 μL HR5-GFP-MybW (25 μM), 1 μL HR3-GFP-MybW (25 μM), 1 μL pdm326 (25 ng/μL), 1 μL Phusion® Polymerase, 10 μL Phusion® HF buffer (5x), 4 μL dNTPs (2.5 mM) and 32 μL MilliQ. The sequences for HR5-GFP-ROCO4, HR3-GFP-ROCO4-new, HR5-GFP-MybW and HR3-GFP-MybW can be found in supplementary table 1.

The PCRs were performed under the following conditions using a Bio-Rad® C1000 touch thermal cycler: an initial 98˚C for 30 seconds, which was followed by 34 cycles of 98˚C for 10 seconds, 60˚C for 30 seconds and 72˚C for 60 seconds which was then followed by a final step of 72˚C for 10 minutes. The presence of PCR product was verified through gel electrophoresis using 1% agarose gels, where a band of around 900 bp implied successful amplification. The PCR product was then purified using the Nucleospin® Gel and PCR Clean-up kit following manufactures protocol. (Machery-nagel, 2023)

Strains & cell culture

AX2 and *Roco4 null* were cultured at 21 ˚C on culture dishes or in shaking culture in HL-5 medium and chloramphenicol (34 μg/mL). Transformants were cultured at 21 ˚C on culture dishes in medium containing neomycin (10 μg/mL) as a selection marker). Some of the transformants also received blasticidin (10 μg/mL) as a second selection marker, while others were cultured on SM agar plates with *Klebsiella aerogenes*.

Transfection

Around $2*10^7$ Dictyostelium cells were transfected with 3 μL of plasmid DNA per plasmid (354 – 455 ng/μL). Conditions that included an insert were also transfected with 6 μL of either blast (36.9 – 68.5 ng/μL) or GFP DNA (28 – 45 ng/μL). The Dictyostelium cells were transfected according to the following conditions: *Roco4_55* knockout*, Roco4_55*+ *Roco4_56* + *Roco4_60* knockout*, Roco4_55 knockout* + *blast, Roco4_55* + *Roco4_56* + *Roco4_60 knockout* + *blast, Roco4_55* + *GFP, Roco4_55* + *Roco4_56* + *Roco4_60* + *GFP*, *MybW* knockout, *MybW* knockout + blast and *MybW* + GFP. The cells were transfected by electroporation (1 pulse: 500 V, 50 μF, 13 Ω) using the BTX® Electro cell manipulator 600. After transfection all plates received neomycin (10 μg/mL) as a selection marker.

Selection of transformants

The full transfection and selection procedure is shown in Figures 3 – 6.
Two days after transfection and selection with neomycin (10 μg/mL), blasticidin (10 μg/mL) was added as a second selection marker to the plates transfected with blast DNA. For further selection,100 cells from both the knockout (w/o blast) and GFP plates were mixed with 100 μL of klebsiella in LB broth and subsequently spread on SM Agar plates. For each of the klebsiella plates, a back-up plate was kept in culture. The back-up plates did not contain a selection marker.

One week after transfection, all culture plates contained rounded, non-adherent cells with no clonal colonies observed. Similarly, the klebsiella plates showed no clonal colonies. Two weeks after transfection, the cells of the blasticidin-containing plates remained predominantly round and non-adherent and were thus presumably all dead, the cells were subsequently removed from culture.

Despite the blasticidin plates being negative, some of the knockout and GFP plates kept in culture showed clonal colonies. Easily identifiable clonal colonies were picked using a sterile pipette tip and transferred to a 6-well plate containing HL-5 medium. Overgrown plates were transferred to SM agar plates with klebsiella. This time, approximately 1000 cells were resuspended in 100 μL of Klebsiella cells in LB broth.

In the following days, after sufficient growth, the cells from the 6-well plate were transferred to 9 cm plates. Simultaneously, clonal colonies identified on the klebsiella plates were picked using a sterile pipette tip and transferred to a 6-well plate containing medium. These were later transferred to 9 cm plates after sufficient growth.

Validation of genome editing

Primers were designed to amplify and sequence the mutated regions of the Dictyostelium genome. The sequences of these primers can be found in supplementary table 2. The culture plates were resuspended in 2 mL of HL-5 medium and pipetted into a 2 mL Eppendorf® tube. The Eppendorf® tubes were centrifuged at max speed after which the supernatant was aspirated leaving the pellet containing cells for PCR. Before PCR, the pellets were placed in a heat block at 96˚ C for 5 minutes and spun down to pellet debris and intact cells. The supernatant was used as template for the PCR.
The PCR mixture for the amplification of the mutated *Roco4* region consisted of; 1 μL ROCO4_FW_genome (25 μM), 1 μL ROCO4_RV_seq (25 μM), 1 μL template (cells), 1 μL Phusion® polymerase, 10 μL Phusion® HF buffer (5x), 4 μL dNTPS (2,5 mM) and 32 μL MilliQ. The PCR mixture for the amplification of the mutated *mybW* region consisted of; 1 μL MybW_FW_genome (25 μM), 1 μL MybW_RV_genome (25 μM), 1 μL template (cells), 1 μL Phusion® polymerase, 10 μL Phusion® HF buffer (5x), 4 μL dNTPs (2,5 mM) and 32 μL MilliQ. The PCRs were performed under the following conditions using a Bio-Rad® C1000 touch thermal cycler: an initial 98˚C for 30 seconds, which was followed by 34 cycles of 98˚C for 10 seconds, 60˚C for 30 seconds and 72˚C for 1 minute and 50 seconds which was then followed by a final step of 72˚C for 10 minutes. The presence of PCR product was verified through gel electrophoresis using 1% agarose gels.

Developmental assay

A developmental assay was performed to assess whether the mutations induced through CRISPR/Cas9 resulted in a specific phenotype after spore development. AX2 cells were used as a wild-type control, while *Roco4 null* cells served as a positive control for the *Roco4* knockouts. Two additional experimental samples were included: AX2 cells transfected with a *Roco4*-GFP plasmid, pdm323, causing overexpression of Roco4, and *Roco4 null* cells also transfected with pdm323, serving as a rescue condition.

Per condition, a full 9 cm plate of cells was washed with PB and centrifuged at 300 g. Subsequently, the supernatant was aspirated, and the pellet of cells was resuspended in 500 μL PB. The resuspended cells were transferred to non-nutrient agar plates already containing 1000 μL of PB to evenly spread out the cell suspension. After 15-30 minutes of settling down, the excess pb was aspirated. The pictures were taken 2 days later using the ZEISS® Stemi SV 11 light-microscope.

Immunofluorescence Assay

For the immunofluorescence assay, $0.8*10^5$ AX2 or *Roco4 null* cells per chamber were seeded in polyl lysine coated IBIDI® chambers and incubated at 21˚C overnight.
The cells were then fed with Texas red zymosan beads (5 beads/cell) for 1.5 hours. Following the feeding, the cells were fixed, permeabilized and blocked, with washing steps in between. Subsequently, the cells were incubated with the primary antibody, Rab8a (PT72), which was diluted to 1:500 in blocking buffer (3% BSA, 0.1% Tween, PB). After another washing step the cells were incubated with the secondary antibody, α-Donkey-anti-rabbit-green fluorophore, which was diluted to 1:400 in blocking buffer (3% BSA, 0.1% Tween, PB). Pictures were taken using an LSM800® confocal

microscope. The entire protocol of the immunofluorescence assay can be found in the supplementary materials.

Flow cytometry

For the flow cytometry assay, $0.5*10^5$ AX2 or *Roco4 null* cells per well were seeded in a flatbottom 96-well plate and incubated at 21 ˚C overnight. The cells were then fed with FITC and/or pHrodo zymosan beads (5 beads/cell) and incubated for 1.5 hours. Each of the conditions was performed in duplicate. Following the incubation step, the cells were washed using pb and transferred to a conical bottom 96-well plate. The plate was then centrifuged at 300 RCF for 3 minutes at 21 ˚ C, after which the plate was washed twice with PB while centrifuging in-between washing steps. Finally, measurements were done using a flow cytometer. The entire protocol of the flow cytometry assay can be found in the supplementary materials.

Results

Using CRISPR/Cas9 to create knockouts and GFP-inserts for *Roco4* & *mybW* in Dictyostelium

In order to create knockouts and GFP-inserts for the *Roco4* & *mybW* genes four different gRNAs were generated. Three of these gRNAs target the 5' end of the *Roco4* gene and the other one targets the 5' end of the *mybW* gene. These gRNAs were all separately fused with ptm1285 plasmids using a BpiI mediated golden gate reaction. Figure 2 depicts the location of the gRNAs in the sgRNA site of the ptm1285 plasmid using Roco4_55 as an example. After validation of successful gRNA integration into the plasmids the constructs were transfected into Dictyostelium cells.

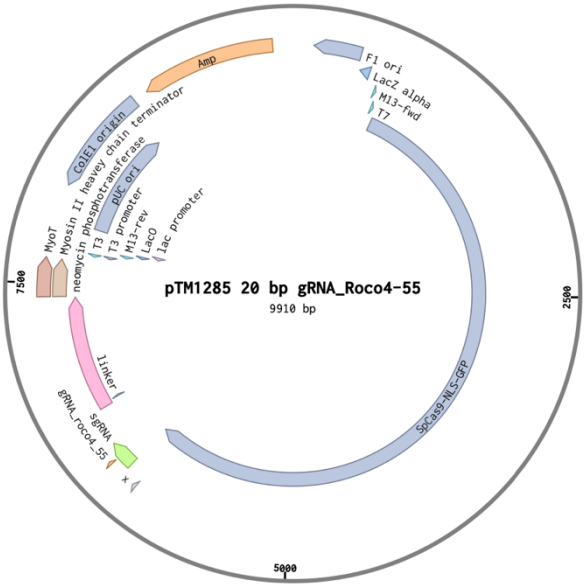

Figure 2 example of CRISP/Cas constructs in ptm1285 plasmids. *Light Brown represents location of gRNAs in the sgRNA site of ptm1285.*

Transfection & selection of transformants

The transfection and selection procedure of the *Roco4* and *mybW* knockouts and GFP-inserts is illustrated in figures 3 - 6. Immediately after transfection, the cells received neomycin as a selection marker which led to a mix of dead and adherent cells. This was followed by further selection using either blasticidin or klebsiella plates. In the end the blasticidin selection resulted in only dead cells and thus showed unsuccessful integration of the blast-cassette. While the klebsiella plates returned negative as well, the back-up plates showed clonal colonies and were picked and cultured to validate successful transfection.

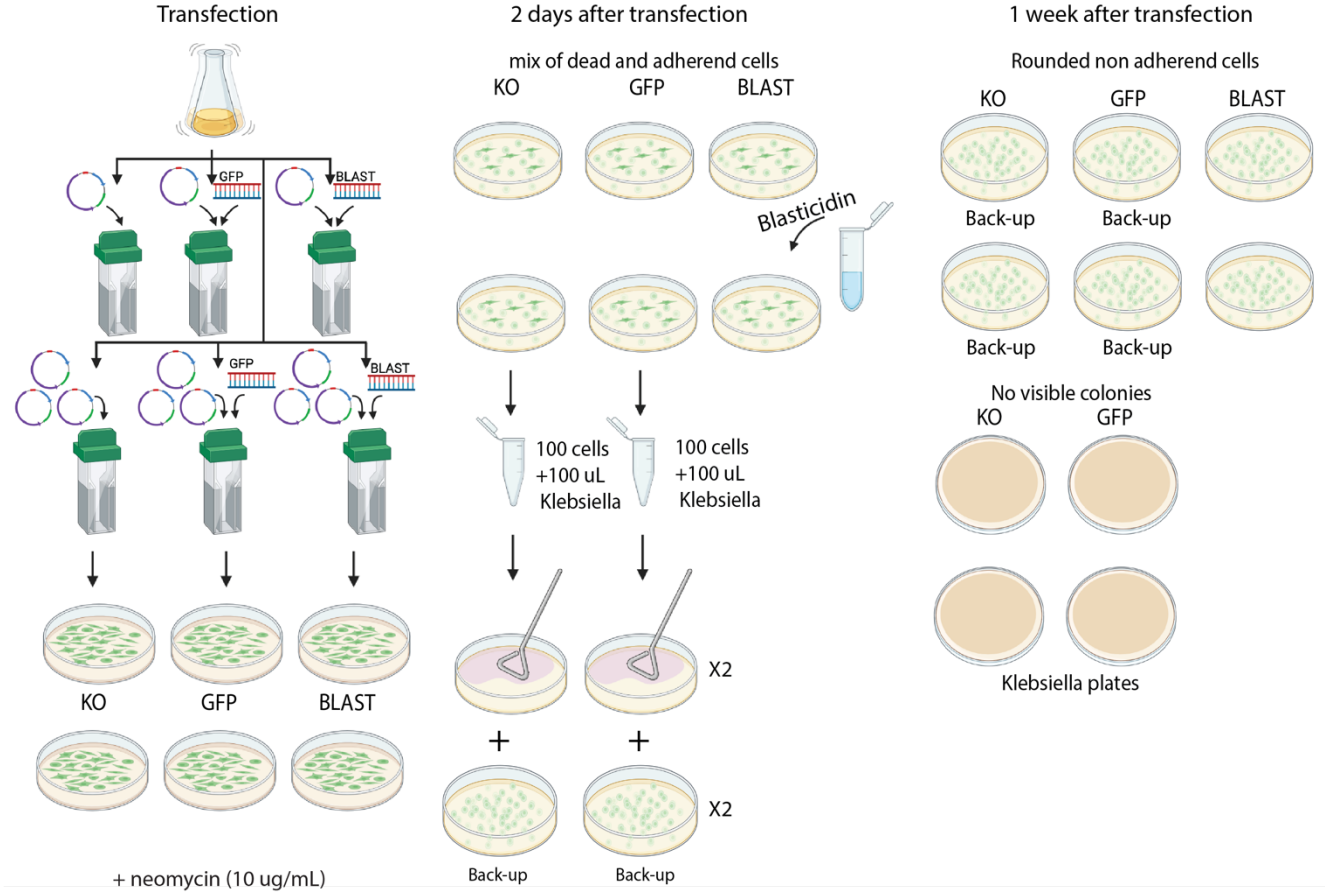

Figure 3 The transfection & selection procedure of the Roco4 knockouts and inserts up until 1 week after transfection.

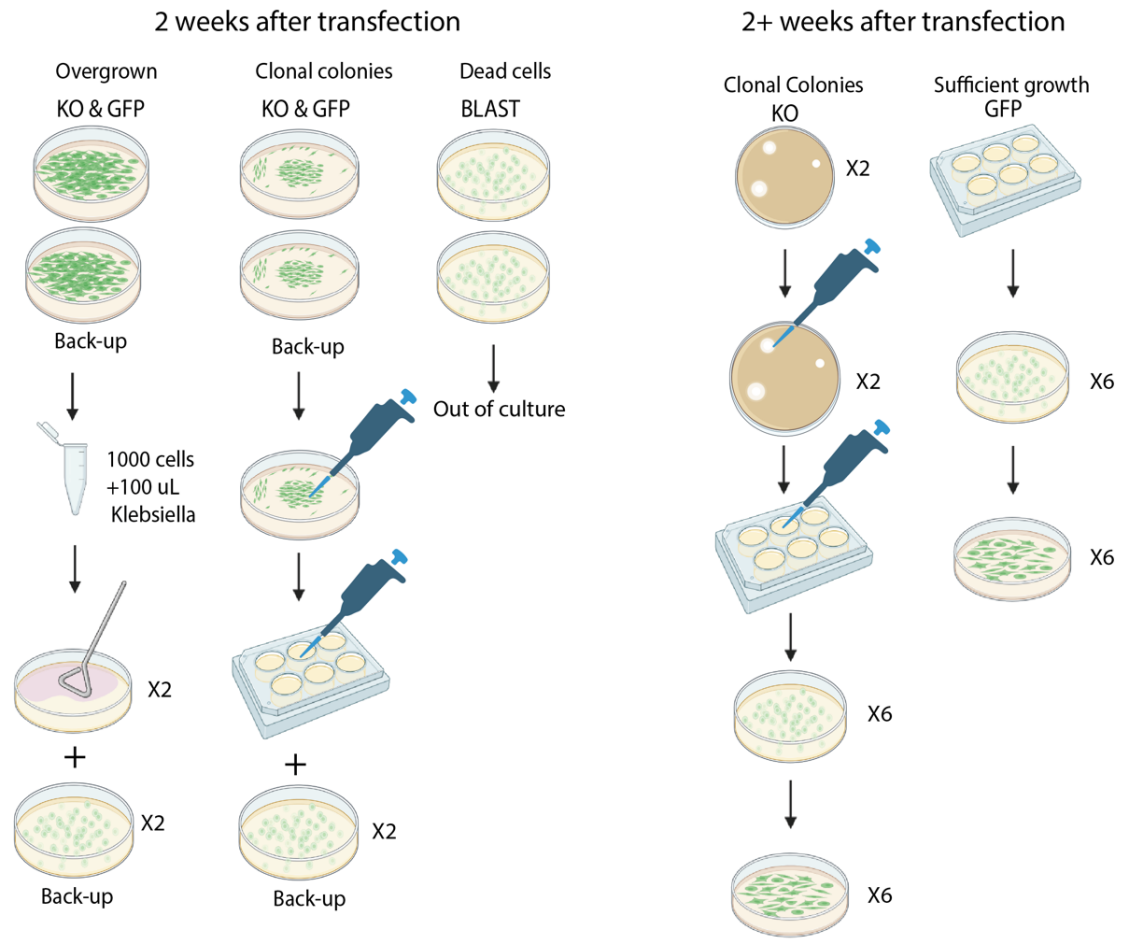

Figure 4 The selection procedure of the Roco4 knockouts and inserts 2 weeks after transfection.

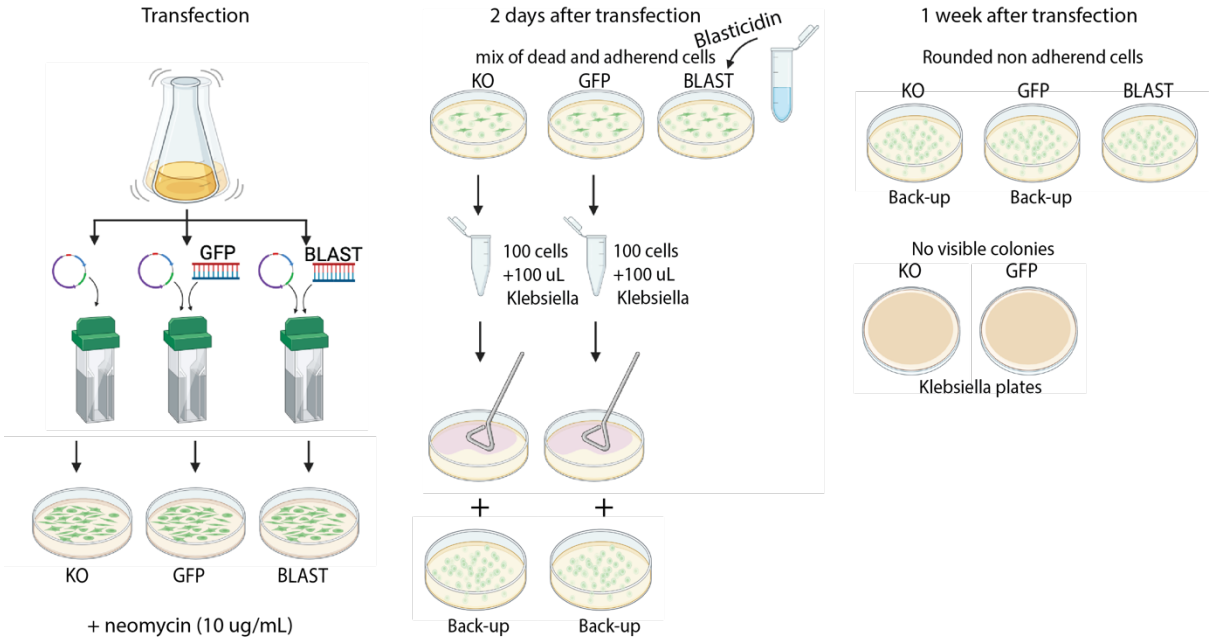

Figure 5 The transfection & selection procedure of the MybW knockouts and inserts up until 1 week after transfection.

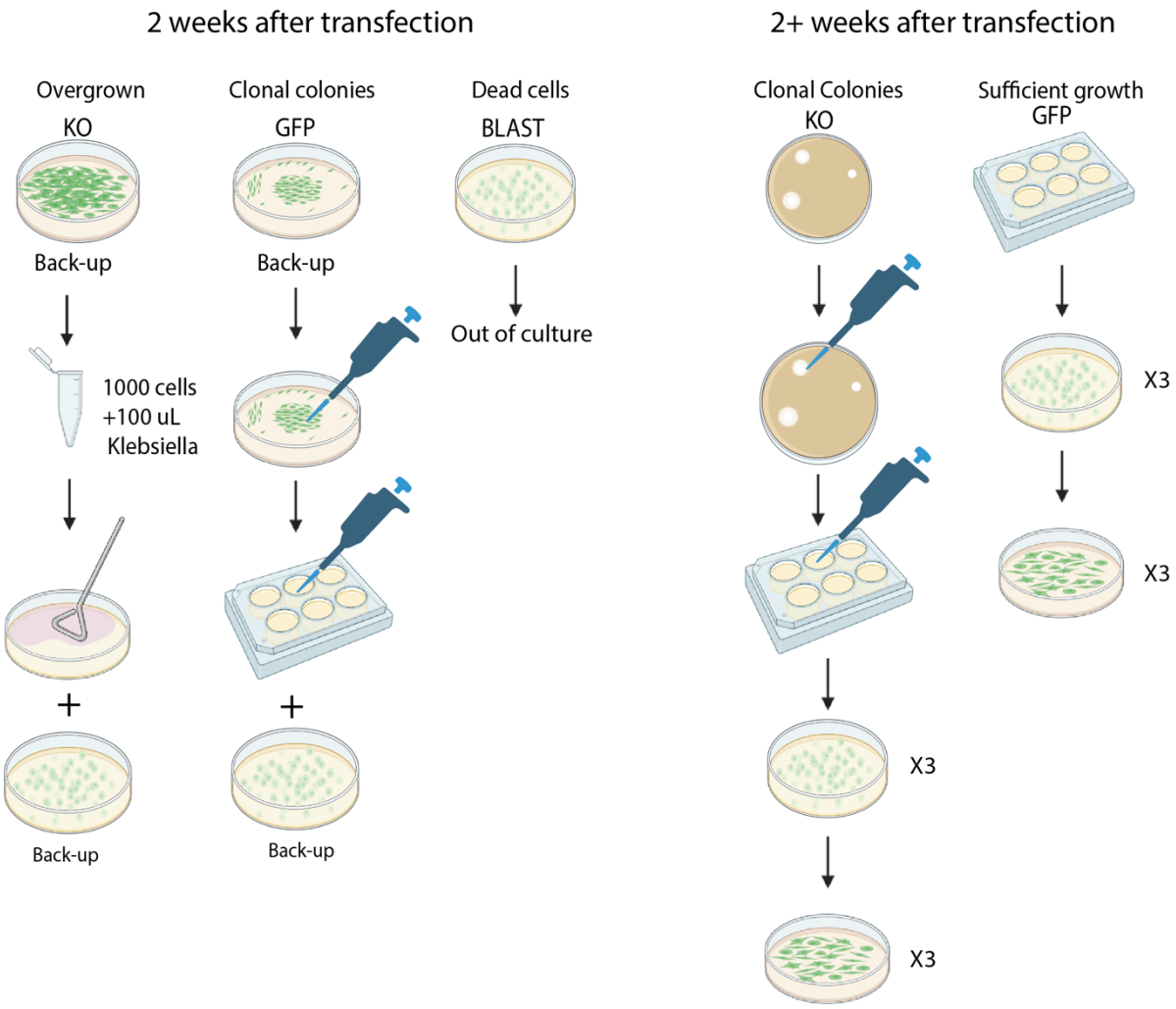

Figure 6 The selection procedure of the MybW knockouts and inserts 2 weeks after transfection.

Validation of Genome Editing

To validate the creation of successful knockouts and GFP-inserts, primers were designed to amplify and sequence the mutated region of the Dictyostelium genome. The presence of PCR product was verified through gel electrophoresis to see if the amplified DNA matched expectations. The results of the gel electrophoresis are depicted in Figures 7 & 8.

Roco4

For the *Roco4* knockout cells it was expected to see a band around 808 bp, while for the *Roco4* GFP cells a band around 1522 bp was expected. However, as shown in figure 7, none of the *Roco4* cell lines showed a band at the expected position. Some faint bands were observed in lanes 4 (figure 7A); 2-4 (figure 7B); and 6 & 7 (figure 7C), but none correspond to the expected bp.

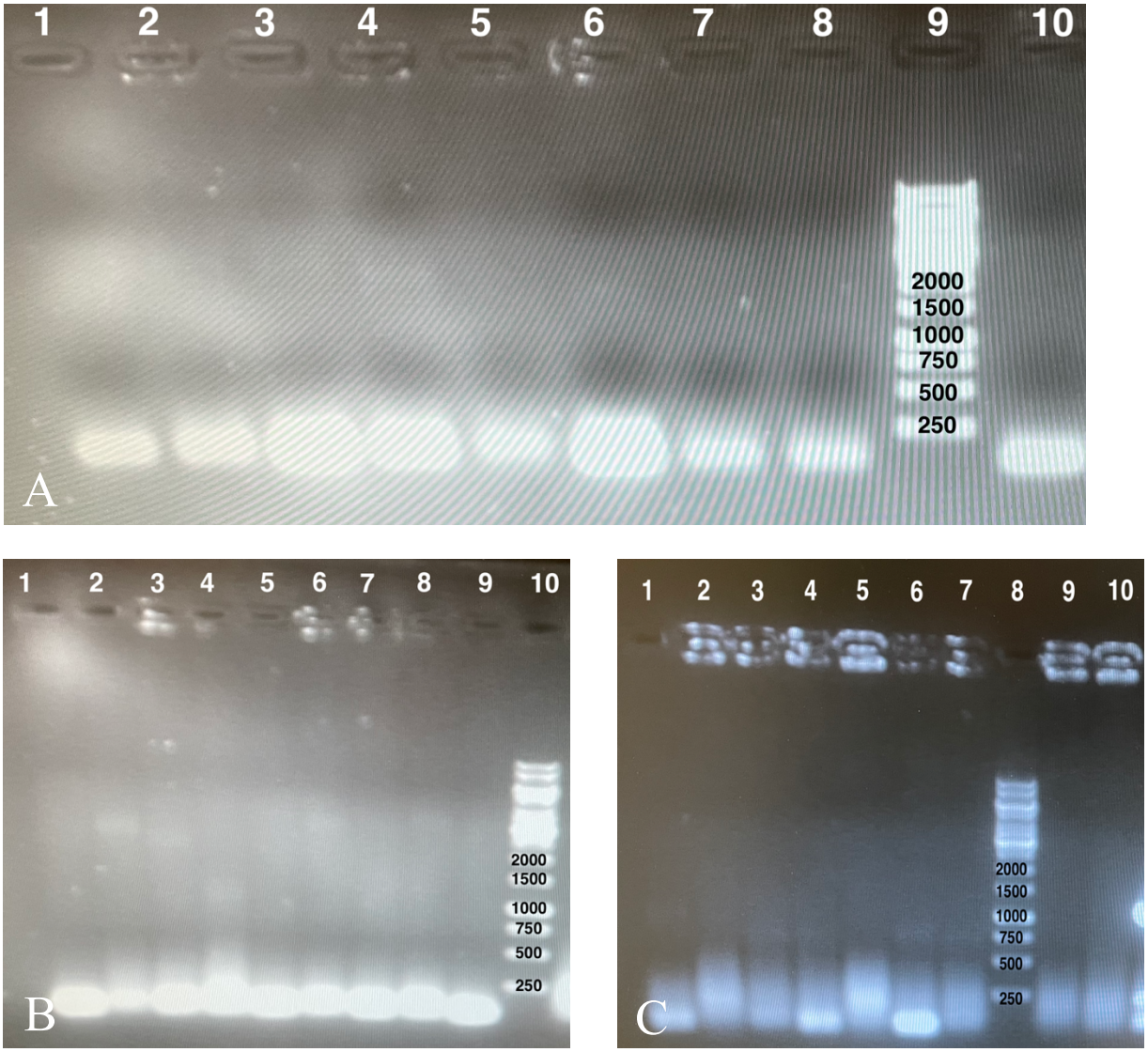

Figure 7 1% Agarose gel electrophoresis of PCR amplified products using Roco4 gene specific primers*. A: Lane 1-4: Roco4 KO, Lane 5-8: Roco4-GFP, Lane 9: 1KB DNA Marker, Lane 10: Roco4-GFP. B: Lane 1-4: Roco4 KO, Lane 5-9: Roco4-GFP, Lane 10: 1KB DNA Marker. C: Lane 1-4: Roco4 KO, Lane 5-7: Roco4-GFP, Lane 8: 1KB DNA Marker, Lane 9-10: Roco4-GFP.*

mybW:

For the *mybW* knockout cells, the expectation was to see a band around 395 bp, while for the *mybW* GFP cells a band around 1109 bp was expected. In figure 8A, lane 5 shows a band between 1000 and 1500 bp which could align with the expected 1109 bp. However, subsequent PCRs did not exhibit this same band. The other *mybW* lanes showed either no band or a band at an unexpected amount of bp.

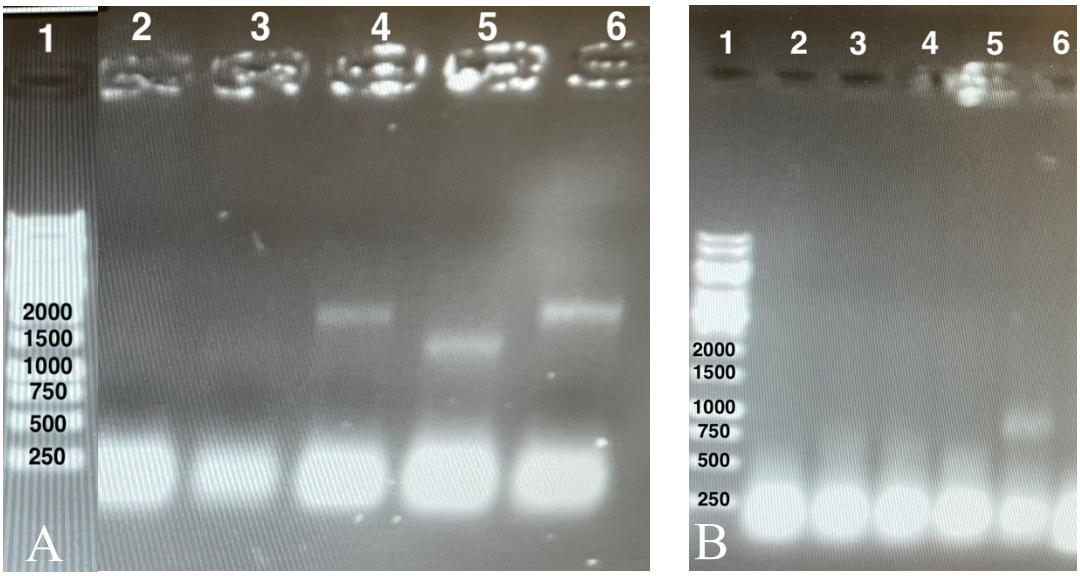

Figure 8 1% Agarose gel electrophoresis of PCR amplified products using mybW gene specific primers*. A: Lane 1: 1KB DNA marker, Lane 2: MybW KO, lane 3-6: MybW GFP. B: Lane 1: 1KB DNA marker, Lane 2: MybW KO, lane 3-6: MybW GFP.*

Since all PCR results returned negative, it is difficult to determine whether the knockouts and GFP-inserts were successful or not. Especially since the same PCR protocol proved successful while using different primers and pre-existing *Roco4 null* strains, suggesting that the issue likely lies with the primers designed for the target genes. In addition to the PCR, an Immunofluorescence assay was used to detect GFP-fluorescence in the transformants with a GFP-insert. However, these results also came back negative, indicating unsuccessful integration of the GFP-insertions into the Dicytostelium genome. Despite these setbacks, there was one last hope of validating successful transformation, the developmental assay.

Investigating cell developmental phenotypes compared to published research

A developmental assay was performed to assess whether the mutations induced through CRISPR/Cas9 resulted in a specific phenotype during and after spore development. In the case of the *Roco4* knockouts, this assay served as verification of successful cloning since *Roco4* knockouts (*Roco4 null*) are known to have a distinct phenotype during and after spore formation. The major phenotypical differences between *Roco4 null* and wild-type cells appear twelve hours after starvation; while wild-type cells are starting to form slugs and their first fingers, *Roco4 null* mounds have mostly transformed into doughnut-shaped structures that last for about 1 to 4 hours. After 16 hours of starvation, some of the *Roco4 null* mounds slowly form their first

fingers, to develop into slugs. However, most *Roco4 null* mounds transform into slugs after 26 hours. These slugs then migrate for many hours before making multiple attempts to culminate, a process that sometimes takes up to 72 hours after the onset of starvation. Eventually, this results in fruiting bodies consisting of spore heads that are located on the agar surface, because their stalk is underdeveloped and not able to lift the spore head into the air. (van Egmond & van Haastert, 2010) Regarding *mybW*, no *mybW* knockouts or GFP-inserts have been developed in Dictyostelium cells as of now, thus no spore development phenotypes have been reported so far.

For comparative analysis, AX2 cells were used as a wild-type control, while *Roco4 null* cells served as a positive control for the *Roco4* knockouts. During the developmental assay, two additional experimental samples were included: AX2 cells transfected with a *Roco4*-GFP plasmid, pdm323, causing overexpression of *Roco4*, and *Roco4 null* cells also transfected with pdm323, serving as a rescue condition. The re-expression of Roco4 in *Roco4 null* cells is known to rescue the *Roco4 null* phenotype, although some of the resulting fruiting bodies have slightly smaller stalks. (van Egmond & van Haastert, 2010) The spores were photographed after 48 hours of starvation using the ZEISS® Stemi SV 11 Light microscope.

The controls, *roco4 null* and AX2, were difficult to distinguish from each other, which can be seen in figure 9 (A1, A2/B1, B2). Contrary to expectations, the distinctive phenotype of *Roco4 null* was not evident. *Roco4 null* did not exhibit an elongated slug phase compared to the AX2 cells. Moreover, both AX2 and *Roco4 null* showed spore heads located on the agar surface, which contradicts the published *Roco4 null* phenotype. No other phenotypes clearly distinguished *Roco4 null* from AX2.

The *Roco4* knockout (7.1, 7.2 & 7.3) spores, depicted in figure 9 (C1 – E2), did not exhibit the specific phenotype that has been established for *Roco4 null* spores. Furthermore, The *Roco4*-GFP (4.1, 4.2 & 4.3) spores, depicted in figure 9 (F1 – H2), did not portray any distinct phenotype compared to the AX2 spores. The overexpressed *Roco4*-GFP and *Roco4*-GFP rescue spores, as shown in figure 9 (I1 – J2), did not exhibit any distinct phenotype compared to the AX2 spores as well. Finally, the *mybW* Knockout & *mybW*-GFP spores, depicted in figure 9 (K1 – O2), showed no distinct phenotypes in comparison with the AX2 cells.

This assay showed that there were no distinctive phenotypes in any of the strains compared to AX2. Since the *Roco4* knockouts did not exhibit the developmental phenotype mentioned in literature it is likely that there were no successful *Roco4* knockouts. However, since the PCR was unable to give a clear indication of whether the target genes were edited or not it is difficult to clarify if the phenotypes seen in the developmental assay were caused by unsuccessful transformation. Nonetheless, at this point in the project there was no time left for troubleshooting the PCR or a second round of transfection and selection. Luckily, the research questions regarding the role of Roco4 in phagocytosis could be answered using the pre-existing *Roco4 null* and wild-type cell strains.

	Overview: 1.6x	Close-up:6x
AX2	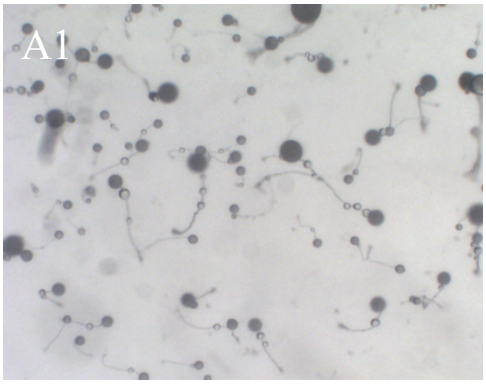	
Roco4 null	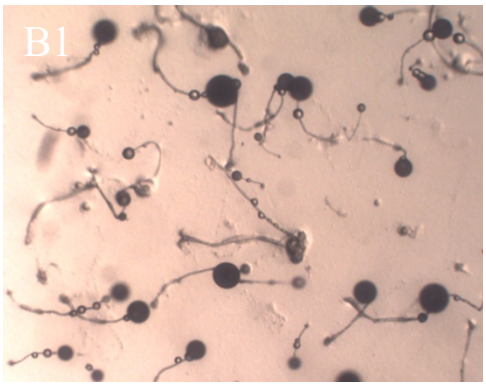	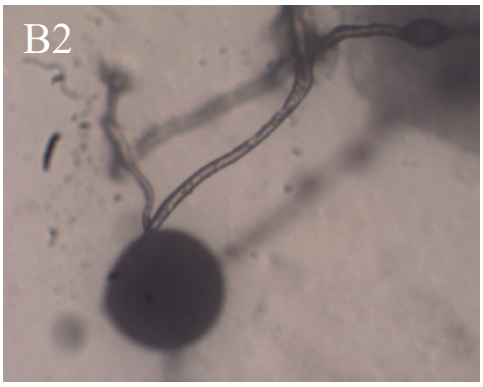
Roco4 KO (7.1)	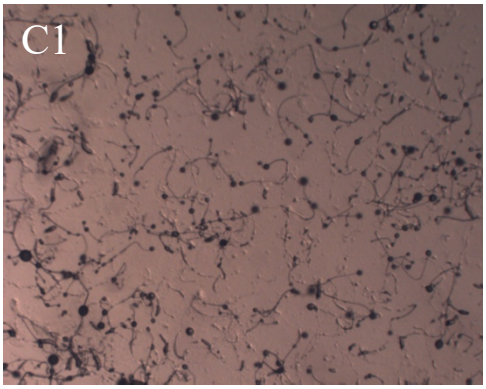	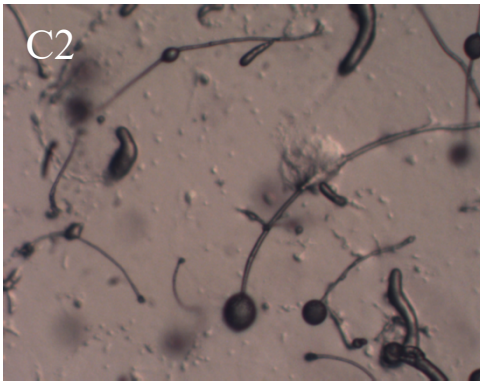
Roco4 KO (7.2)	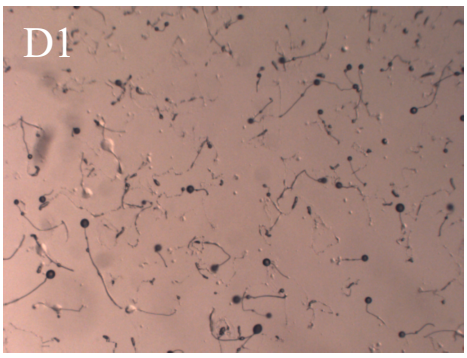	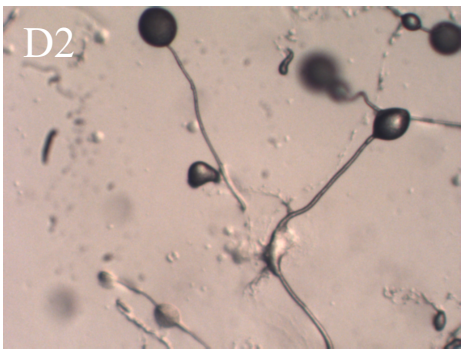

Roco4 KO (7.3)

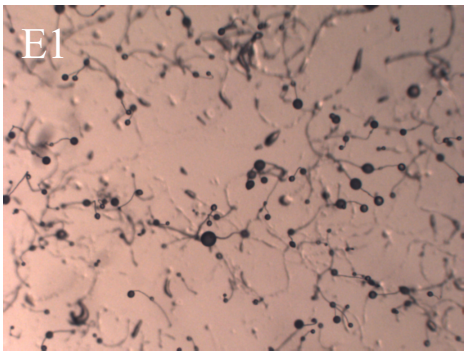

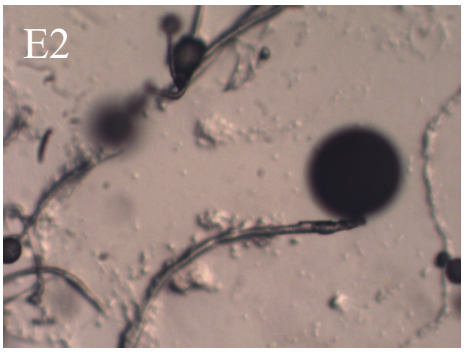

Roco4 GFP (4.1)

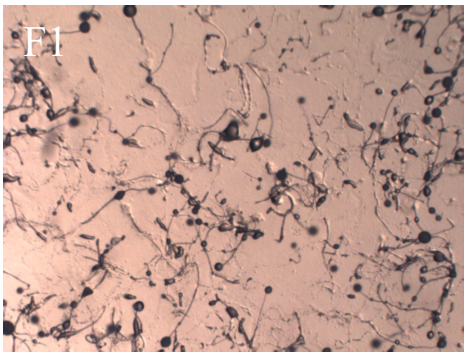

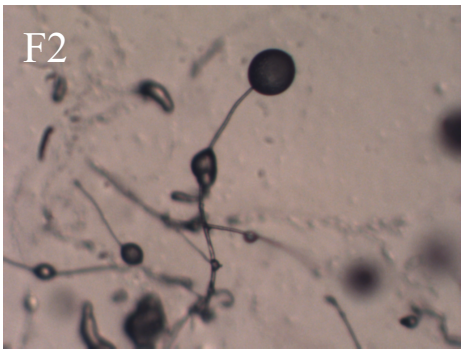

Roco4 GFP (4.2)

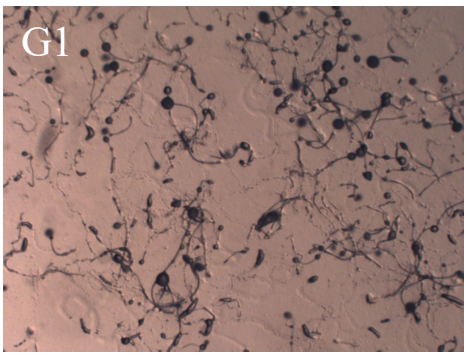

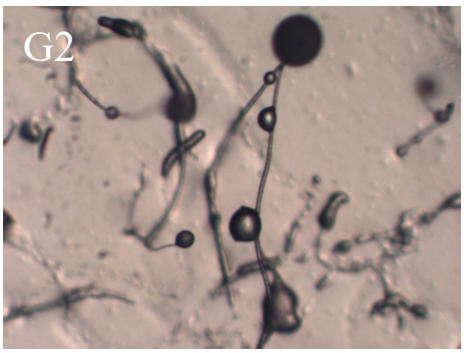

Roco4 GFP (4.3)

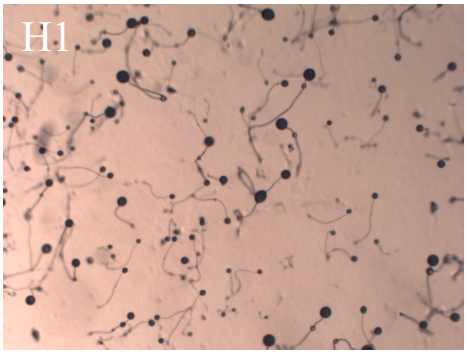

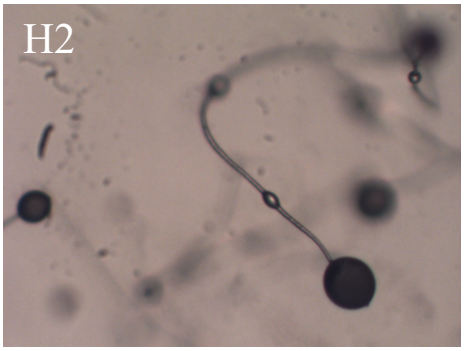

Overexpressed *Roco4* GFP

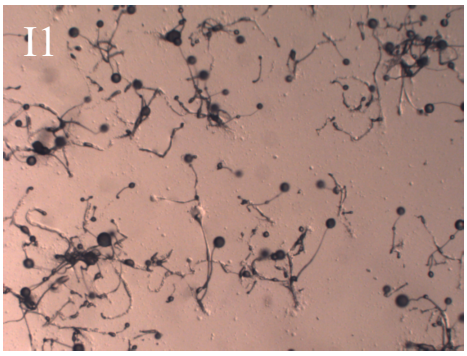

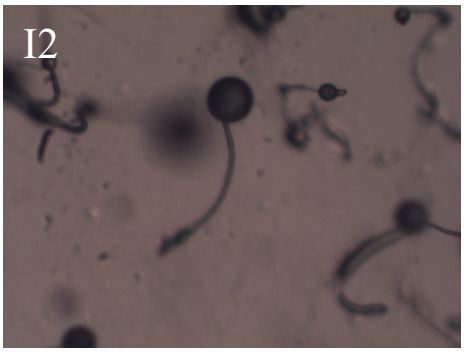

Roco4 null GFP rescue

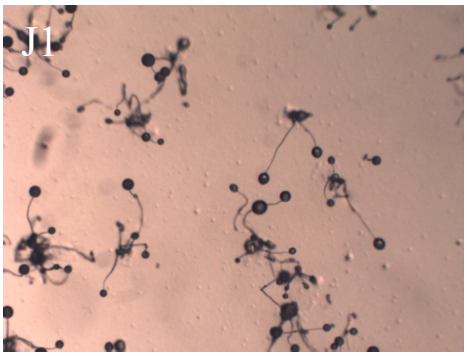

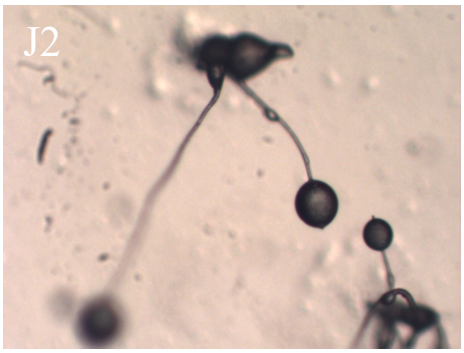

mybW KO

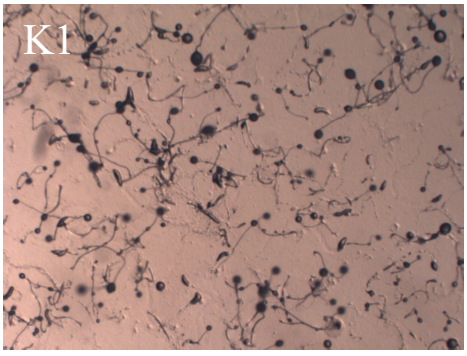

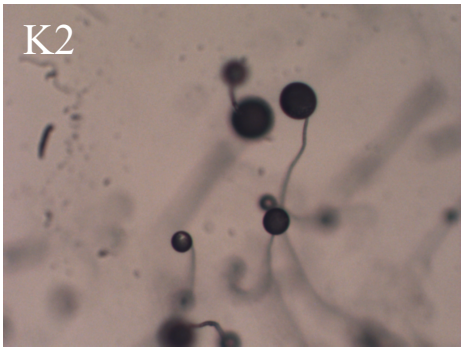

mybW GFP (9.1)

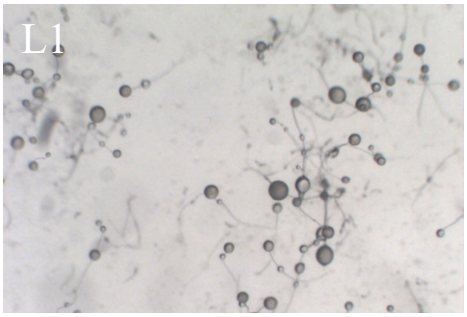

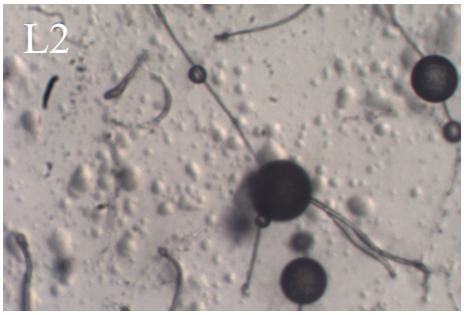

mybW GFP (9.2)

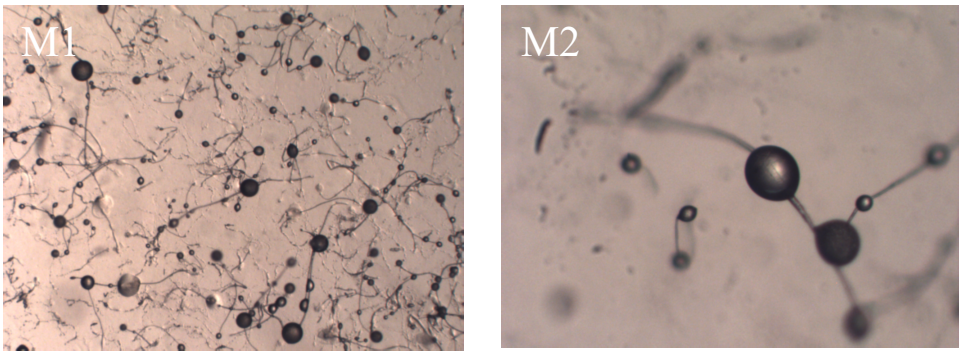

mybW GFP (9.2.2)

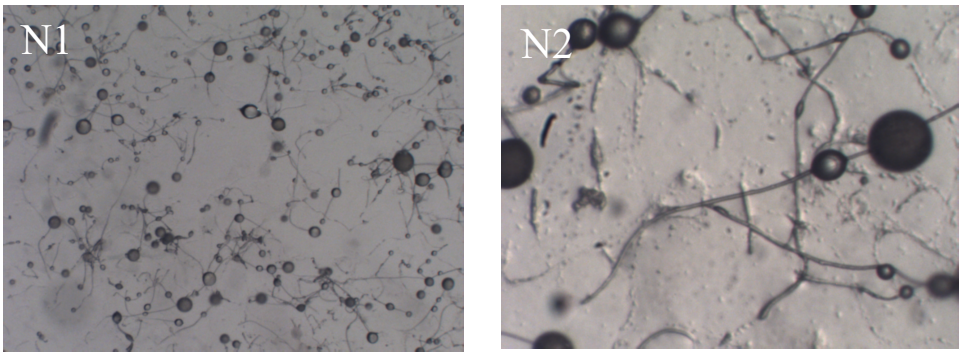

MybW GFP (9.3)

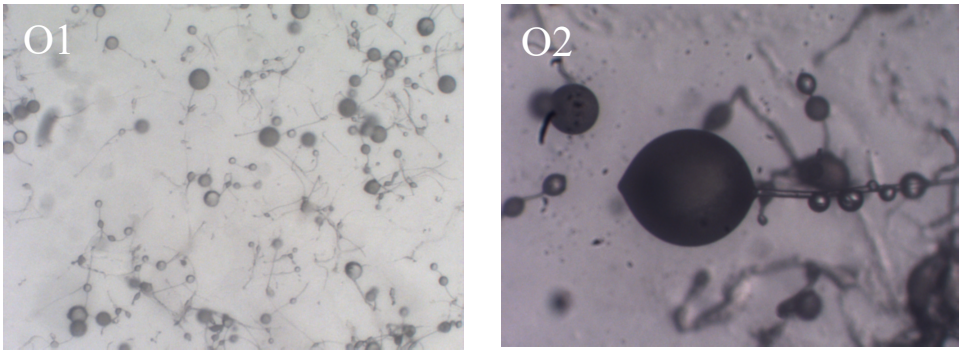

Figure 9 Developmental assay performed on non-nutrient agar plates *for AX2(A1,A2), Roco4 null(B1,B2) , Roco4 KO(C1-E2), Roco4 GFP(F1-H2), Roco4 null rescue(I1,I2), Roco4 GFP overexpressed(J1,J2), MybW KO (K1,K2) and MybW-GFP (L1-O2), pictures were taken after 2 days using a light microscope, all overview pictures have a 1.6x zoom and all close-up pictures have 6x zoom.*

Roco4 phosphorylates Rab proteins during phagocytosis

Roco4 is a homologue of LRRK2. (Gilsbach et al., 2012)
Studies have shown that endogenous LRRK2 phosphorylates Rab proteins, including Rab3, Rab8, Rab10, Rab12, Rab35 and Rab43. (Steger, et al., 2016) (Thirstrup, et al., 2017) Other studies have observed similar phosphorylation of Rab proteins by Roco4. (Rosenbusch, et al., 2021) The Dictyostelium Rab protein family contains a relatively large number of members, including novel proteins like RabA and RabC, as well as proteins that appear to be homologues to mammalian Rabs, including Rab7, Rab11, Rab1, Rab2, Rab8, Rab4 (named RabD), and Rab21 (named RabB). (Rupper & Cardelli, 2001)

In this experiment we aimed to assess the cross-reactivity of the mammalian Rab8 antibody in Dictyostelium cells via an immunofluorescence assay. At the moment, no antibodies targeting the Rab proteins in Dictyostelium are available. However, there are antibodies aimed at the Rab proteins in mammalian cells. One of those antibodies is the phospho Rab8 antibody pT72 Rab8a, which binds phosphorylated Rab8a. This antibody is known to be unspecific which could prove helpful for detecting Rab proteins in Dictyostelium. As a second objective, this experiment aimed to give further insight into the phosphorylation of Rabs by *Roco4* by visualizing this process.

The immunofluorescence assay was performed using the cells of Gargi Ahuja.
AX2 cells were used as a wild-type control, while *Roco4* null cells were used as the experimental sample. The *Roco4 null* cells were created by Wouter van Egmond. (van Egmond & van Haastert, 2010)

Examples of the images used for quantification are depicted in figure 10.
In these images, the violet represents the fluorescence emitted by the zymosan beads, which when taken up by a cell represents a phagosome, the turquoise represents the fluorescence from the secondary antibody and consequently indicates the presence of phosphorylated Rab proteins. The phagosomes shown in figure 10 are considered positive when there is a heightened intensity of the turquoise fluorescence around the phagosomes, indicating localization of phosphorylated Rabs, as depicted in figure 10E-G.

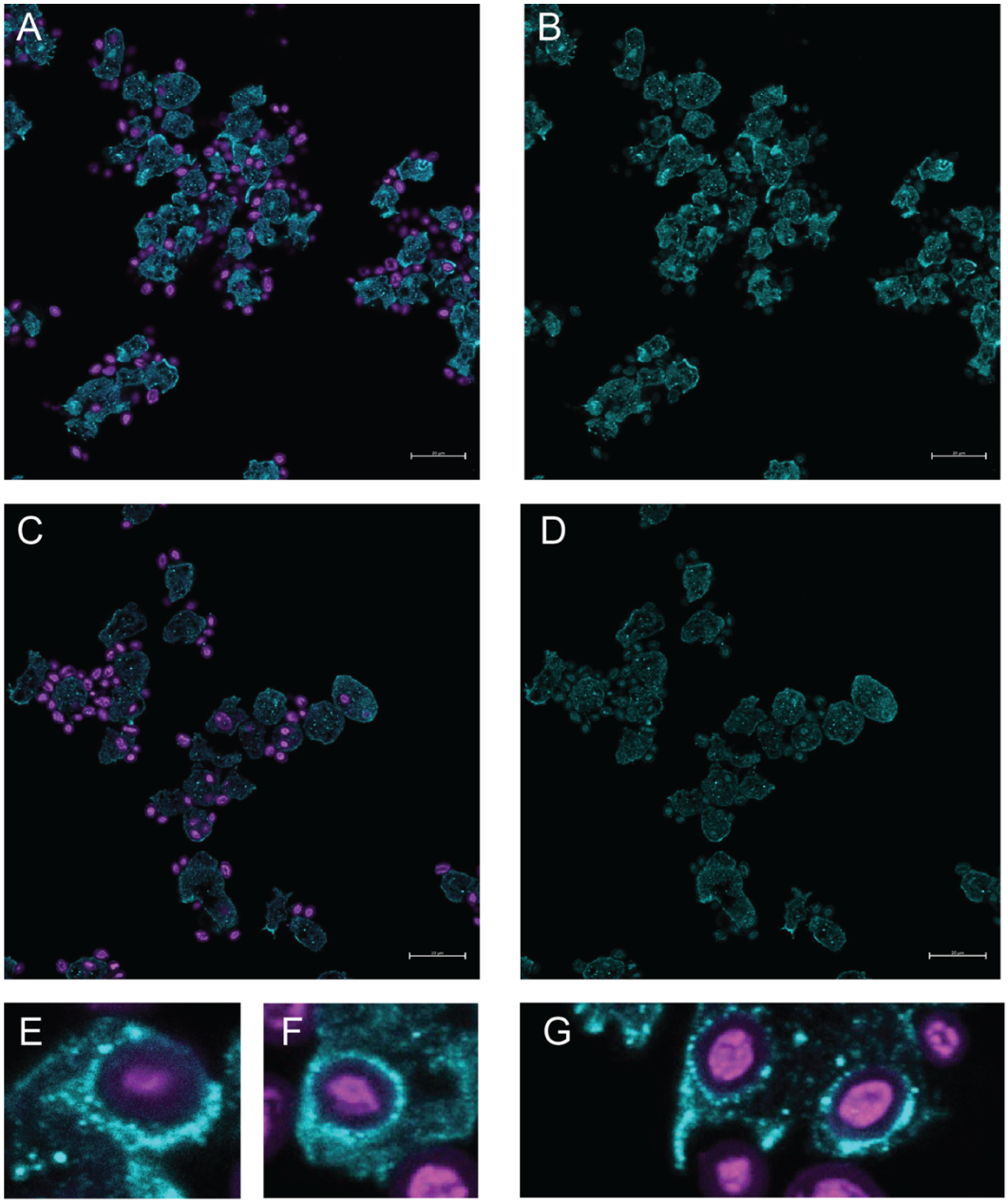

Figure 10 Confocal images of AX2 and Roco4 null cells incubated with zymosan beads for 1.5 hours*. The primary antibody was pT72-Rab8, targeting phosphorylated Rab proteins. Violet represents the fluorescence of the zymosan beads, turquoise is the fluorescence of the secondary antibody. A: AX2 cells with both violet and turquoise channels, B: AX2 cells with just the turquoise channel, C: Roco4 null cells with both violet and turquoise channels, D: Roco4 null cells with just the turquoise channel, E-G: Close up of AX2 cells with localization of phosphorylated Rabs around the phagosomes.*

Figure 11 presents the total percentage of positive phagosomes for both AX2 and *Roco4 null* cells across all images. As mentioned before, phagosomes were considered positive when there was localization of phosphorylated Rabs around the phagosome.

As shown in Figure 11, the wild-type cells had a higher percentage of positive phagosomes than the *roco4 null* cells. Which means that a higher number of phagosomes in the wild-type cells showed localization of phosphorylated Rabs around the phagosomes.

Figure 12 presents the number of cells across all images having taken up a certain amount of zymosan beads for both wild-type and *Roco4 null* cells. This showed that *Roco4 null* cells took up more zymosan beads than the wild-type cells.

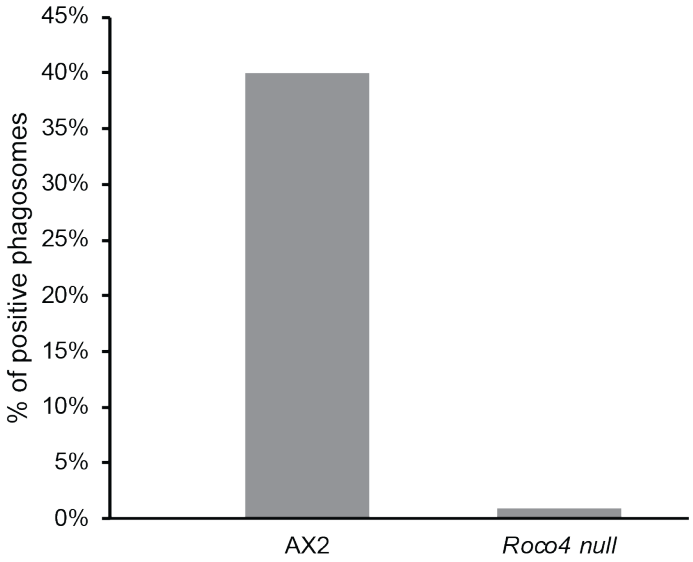

Figure 11 Bar graph of the percentage of positive phagosomes relative to the total amount of phagosomes in AX2 and Roco4 null cells. *Positive phagosomes are phagosomes with localization of phosphorylated Rab proteins. AX2 and Roco4 null cells were incubated with zymosan beads for 1.5 hours and were tagged by the pT72 Rab8 antibody. The amount of phagosomes & positive phagosomes were counted using theLSM800® Confocal microscope.*

This assay showed that the mammalian pT72 Rab8a antibody could be a helpful tool for visualizing Rab protein phosphorylation by Roco4, as there was binding of Rab proteins as displayed in figure 10. Moreover, this assay showed that there was a higher amount of localization of phosphorylated Rab proteins around the zymosan beads within the wild-type cells than in the *Roco4 null* cells. This indicates that Roco4 plays a role in phagocytosis via phosphorylating Rabs in Dictyostelium cells. Lastly, this assay showed that the *Roco4 null* cells had a higher uptake of zymosan beads compared to AX2 cells. Indicating that Roco4 plays a role in phagosomal uptake.

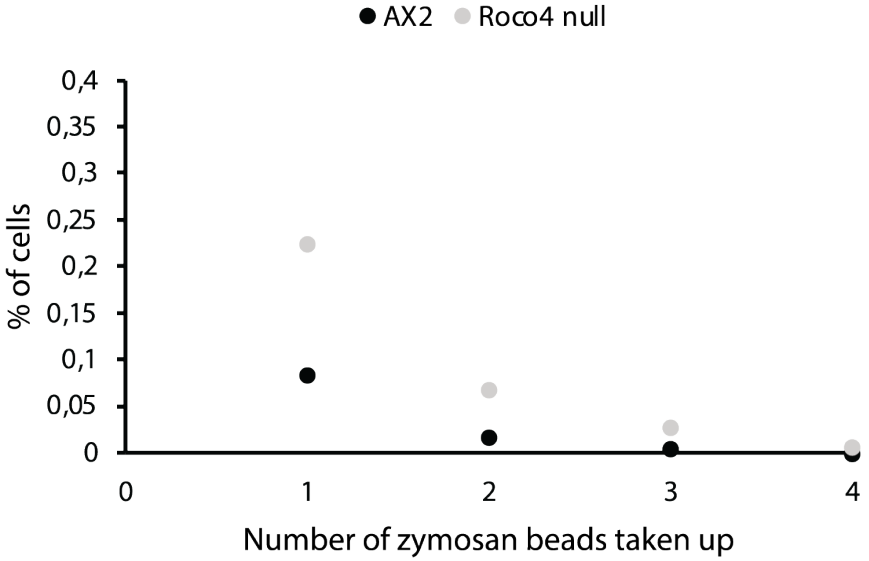

Figure 12 Scatter plot of the number of AX2 and Roco4 null cells containing a certain amount of phagosomes. *AX2 and Roco4 null cells were incubated with zymosan beads for 1.5 hours and were tagged by the pT72 Rab8 antibody. The amount of phagosomes in each cell was counted using theLSM800® Confocal microscope.*

Roco4 plays a role in phagosomal uptake and maturation

LRRK2 has been shown to play a role in phagosome maturation by multiple studies. One study showed that LRRK2 negatively regulates phagosome maturation (Härtlova, et al., 2018). Another study reported that LRRK2 is recruited to maturing phagosomes and is required for recruitment of Rab8 and Rab10. (Lee, et al., 2020) LRRK2 has also been shown to interact with various Rab GTPases, including Rab8a and Rab7L1. (Kuwahara, et al., 2016) (Steger, et al., 2016) Interestingly, Rab8a, among other Rab proteins, has been shown to be important for phagosome maturation (Hanadate, et al., 2016) (Yeo, et al., 2016) On top of that, LRRK2 has been shown to not be involved in initial uptake of bioparticles. (Lee et al., 2020)(Härtlova et al., 2018) Since Roco4 is a homologue of LRRK2 and has shown to interact with Rab proteins the expectation is that *Roco4* also plays a role in phagosome maturation in Dictyostelium cells.

The objective of the flow cytometry experiment was to observe the difference in phagocytosis between wild-type and *Roco4 null* cells, aiming to provide insights into the role of Roco4 in the phagosmal uptake and maturation. This experiment was performed in duplicate by Gargi Ahuja.

Flow cytometry data-analysis, including gating and statistics, was performed using FCS® express software as depicted in the figures below. In the initial gating step, side scatter height was plotted against forward scattered height to distinguish Dictyostelium cells from other debris. Subsequently, in the second gating step, the forward scatter area was plotted against the forward scatter height to select single cells. In the third gating step, the forward scatter area was plotted against the compensated FITC intensity levels to select cells positive for FITC. Finally, In the last gating step, the forward scatter area was plotted against the PE (pHrodo) intensity levels to select cells positive for pHrodo. The experiment was performed in duplicate to allow for statistical testing. A Two-tailed heteroscedastic t-test was performed to test the statistical significance of both the difference in FITC and pHrodo intensity levels.

The FITC levels show the uptake of the zymosan beads, while the pHrodo levels indicate the maturation of the phagosomes, as late-stage phagosomes have lower pH levels, which leads to rapid increase of pHrodo fluorescence.

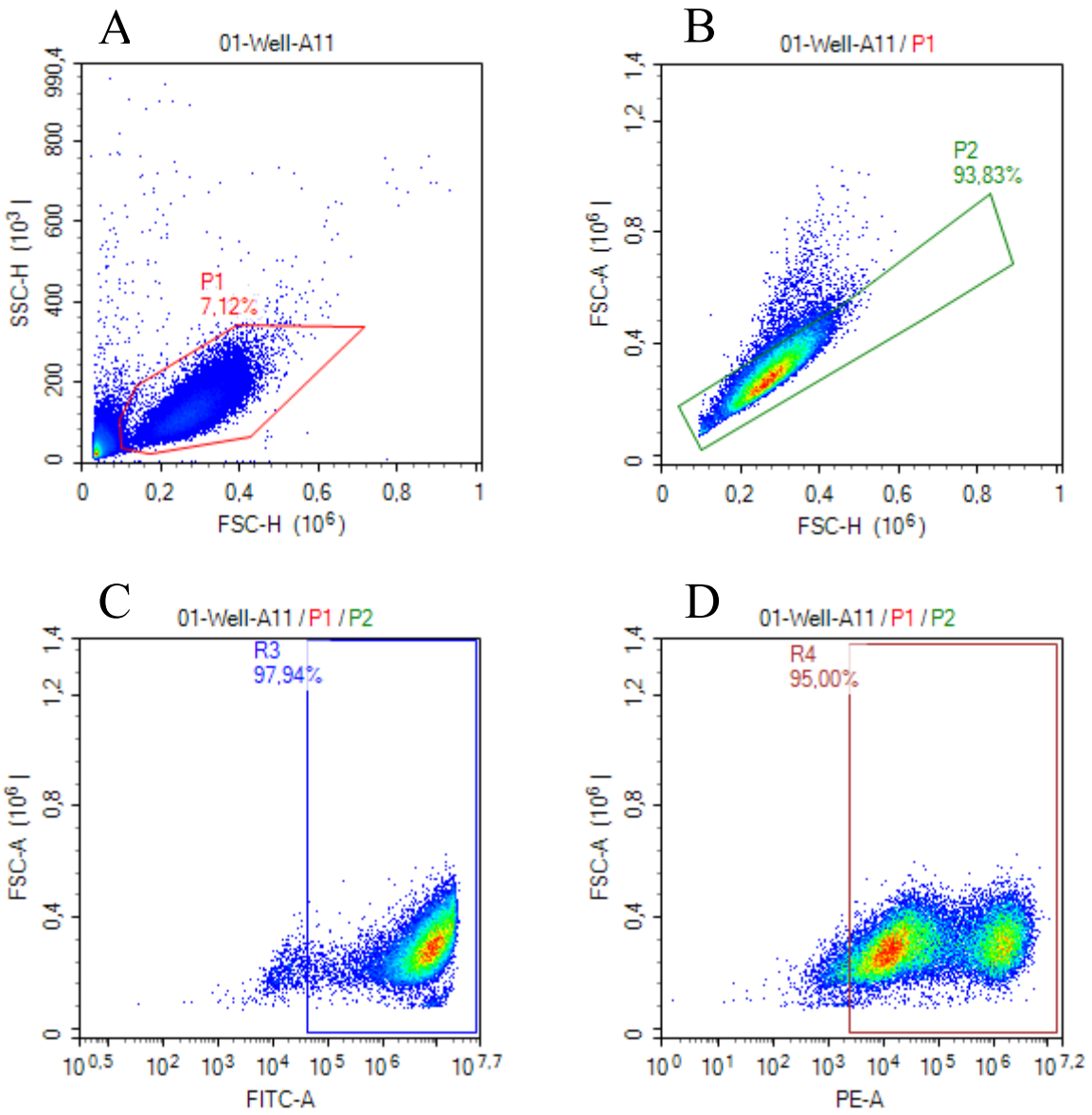

Figure 13 Gating steps flow cytometry analysis using FCS express software. *The same gating was applied to all wells, Well A11, depicted in this figure, serves as an example. Well A11 contained Roco4 null cells incubated with both FITC and pHrodo for 1.5 hours. A) The initial gating step, side scatter height against forward scattered height selecting for dictyostelium cells. B) The second gating step, forward scatter area against forward scatter height, selecting single cells. C), the third gating step, the forward scatter area against the compensated FITC intensity levels. D) the last gating step, forward scatter area plotted against the PE (pHrodo) intensity levels.*

The average FITC intensity levels of the wild-type and *Roco4 null* cells are depicted in figure 14. The FITC levels in the wild-type cells were significantly higher than in the knockout cells with a p-value of 0.026. This indicates that *Roco4* is involved in the uptake process during phagocytosis.

The average pHrodo intensity levels are depicted as the percentage of pHrodo intensity relative to the average FITC Intensity level and can be seen in figure 15. The pHrodo levels were significantly higher in the *Roco4 null* cells than in the wild-type cells with a p-value of 0.039. This indicates that *Roco4* plays a role in phagosomal maturation.

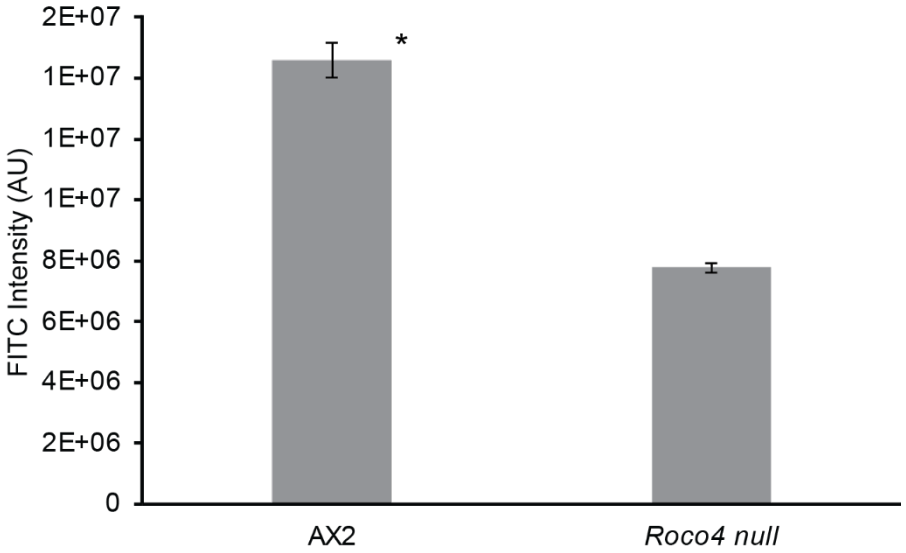

Figure 14 Bar graph of the average measured FITC intensity levels for AX2 and Roco4 null cells. ** P-value=0.026. Error bars represent the standard deviation between the different measurements for that specific cell line.*

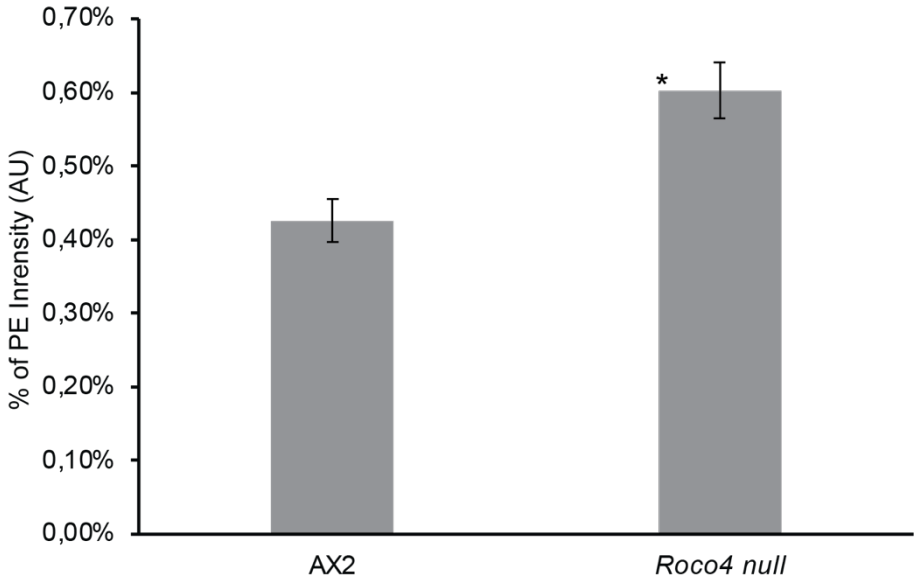

Figure 15 Bar graph of the average PE (pHrodo) intensity levels relative to the average Fitc levels for AX2 and Roco4 null cells. **P-value=0.039. Error bars represent the standard deviation between the different measurements for that specific cell line*

Discussion

Project aim and major findings

The aim of this project was to implement the CRISPR/Cas9 system for Dictyostelium in the cell biochemistry lab using Roco4 and mybW as the model genes, ultimately leading to the creation of knockouts and GFP-inserts for both genes. The *Roco4* knockouts and GFP-inserts would then serve to give insight into the role of Roco4 during phagocytosis. The main questions were whether it was possible to visualize Rab protein phosphorylation by Roco4 during phagocytosis and if Roco4 plays a role in phagosomal uptake and maturation.

In the end, no successful CRISPR/Cas9 knockouts or GFP-inserts were generated for either *Roco4* or *mybW*. Consequently, the assays required to answer the questions surrounding the role of Roco4 in phagocytosis were performed using the pre-existing *Roco4 null* cell line. The immunofluorescence assay showed that it is possible to visualize Rab phosphorylation by Roco4 in Dictyostelium cells by utilizing the pT72 Rab8a antibody. Subsequently, the flow cytometry assay showed that Roco4 is involved in the uptake process during phagocytosis and plays a role in phagosome maturation.

Failed creation of CRISPR/Cas9 knockouts/GFP-inserts for *Roco4* and *mybW*

No successful knockouts or insertions were identified. Due to the PCRs inconclusive results, it is difficult to report whether the targeted regions of the genome were effectively manipulated. Currently, it is unclear what lead to these unexpected results, but it is most likely related to the primers for the target genes. Especially, since the same protocol proved successful using other primers and the pre-existing wild-type and *Roco4 null* cell lines. The bands located at unexpected heights could be the result of off-target amplification due to the high number of repeating sequences in the Dictyostelium genome. However, the primer sequences were blasted against the Dictyostelium genome to limit this problem. Thus, the precise cause of the unexpected bands remains uncertain.

The developmental assay provided further insight on the success rate of the CRISPR/Cas9 reaction and selection process. This assay showed that none of the strains exhibited any distinctive phenotypes compared to AX2. Thus, it is likely that there were no successfully generated knockouts or GFP-inserts. Especially since *Roco4 null* is known to have a distinct phenotype. (van Egmond & van Haastert, 2010) However, this phenotype was also absent in the *Roco4 null* control compared to AX2. The similarity in phenotypes between both controls undermines the credibility of the results, especially since the transformants were derived from the same AX2 strain. During later testing by Gargi, it was revealed that the AX2 strain was actually a mixture of AX2 and *Roco4 null* which explains the similarities between the controls, as well as the similarities between the transformants and the controls since these were derived from the same AX2 strain.

Assuming that there were no successfully generated knockouts and GFP-inserts for both *Roco4* or *mybW*, it is probable that certain aspects of the transfection and

selection procedure caused this outcome. During the transfection, some conditions contained a blast insert. The blast DNA was amplified from a plasmid and then purified. However, after purification the concentration and purity of the blast PCR product was quite low. The lower concentration and purity of the blast DNA during transfection likely reduced the chances of successful integration which ultimately led to the result of no viable *Roco4* and *mybW* knockouts with blast insert.

The knockouts (without blast) and GFP inserts relied solely on the klebsiella plates for further selection as they lacked a second selection marker. Initially, 100 cells from each knockout (without blast) and GFP insert cell strain were transferred to klebsiella plates, yet no clonal colonies were observed. It is plausible that transferring a larger number of cells (200-500) might have increased the likelihood of clonal colony formation. While only 100 cells were initially transferred, the remaining cells were maintained in culture. However, due to the absence of a selection marker there was a higher chance of non-mutated cells outcompeting the mutated cells.

Furthermore, the *mybW* knockout cell strains being unsuccessful could be attributed to this mutation not being viable. KNL2 plays a role cell in cell division (Cheeseman & Desai, 2008), and since *mybW* is a homolog of KNL2, it might be a necessary factor for cell division in Dictyostelium. Thus, making a knockout of this gene non-viable.

Roco4 phosphorylates Rab proteins

Because of its association with LRRK2, which is known to phosphorylate Rab proteins (Steger et al., 2016b; Thirstrup et al., 2017), the expectation was that Roco4 would phosphorylate Rab proteins as well. As expected, the immunofluorescence assay showed that Roco4 phosphorylates Rab proteins in Dictyostelium cells, which is in line with previous research (Rosenbusch, et al., 2021). Additionally, this assay showed that it is possible to visualize this process using the pT72-Rab8 antibody. Besides its involvement in Rab phosphorylation, this assay showed that Roco4 plays a role in phagosome uptake since there was a higher uptake of zymosan beads in wild-type cells compared to *Roco4 null* cells. Given that LRRK2 is involved in vesicular trafficking (Cookson, 2016) (Galatsis, et al., 2014), the phosphorylation of Rab proteins by Roco4 suggests a potential role for Roco4 in vesicular trafficking pathways similar to LRRK2. Notably, since Rab proteins are involved in phagosome maturation (Vieira, et al., 2002) and are phosphorylated by Roco4, it is plausible that Roco4's Rab phosphorylation contributes to phagosome maturation in Dictyostelium. To validate Roco4's involvement in phagosome maturation and further investigate its role in phagosomal uptake a flow cytometry assay was performed.

Roco4 plays a role in phagosomal maturation and uptake

Regarding the Role of Roco4 in Phagosome maturation, it was expected that Roco4 would be an important factor in stimulating phagosome maturation since its homologue LRRK2 has been reported to recruit Rab proteins to phagosomes such as Rab8a and Rab7L1, which are known to play an important role in phagosome maturation.

(Kuwahara et al., 2016; Steger et al., 2016a) The results of the flow cytometry assay confirmed that Roco4 is an important factor in phagosome maturation.

The involvement of Roco4 in phagosome maturation was indicated by the significantly higher pHrodo levels in the *Roco4 null* cells. One possible explanation for this observation could be that the *Roco4 null* cells might not be able to process the phagosomes further than a certain stage due the Rab proteins not being phosphorylated. Currently no studies have proven this exact claim, however the inhibition of Rab7l1 by mycobacterial PknG has shown to hinder phagosome-lysosome fusion in mammalian macrophages and thus affects phagosome maturation. If Rab proteins are not phosphorylated, they may become as dysfunctional as if they were inhibited, leading to a comparable impact on phagosome maturation. Another possible explanation could be that the *Roco4 null* phagosomes undergo accelerated maturation compared to the AX2 phagosomes. And are thus measured at an already later stage than the AX2 phagosomes. This hypothesis is supported by a study reporting that LRRK2 negatively impacts phagosome maturation. (Härtlova et al., 2018)

The flow cytometry assay also showed that the uptake of zymosan beads was higher in wild-type cells than in *Roco4 null* cells, suggesting that Roco4 plays a role in phagosomal uptake. Previous research has shown that knocking down Rabs in mammalian macrophages disrupted phagocytosis prior to phagocytic cup closure. (Yeo, et al., 2016) Thus, Rab proteins not being phosphorylated by Roco4 might disrupt their function and have a similar effect on phagosomal uptake. Currently, no other studies have reported on Roco4's effect on the uptake process. However, LRRK2 has been shown to not be involved in initial uptake of bioparticles. (Lee et al., 2020) (Härtlova et al., 2018) Which due to the homology between Roco4 and LRRK2 contradicts the findings of this project. The reason for this difference is unclear but could be attributed to it being a Dictyostelium-specific function.

What is interesting is that the uptake results of the flow cytometry assay contradict the uptake results of the immunofluorescence assay. The flow cytometry assay showed that there was a higher uptake of zymosan beads in the wild-type cells while the immunofluorescence assay showed that there was a higher uptake of zymosan beads in the *Roco4 null* cells. This could be attributed to observer bias since the phagosomes of the immunofluorescence assay were all manually counted of 2D images, while during the flow cytometry assay the fluorescence levels were measured by a flow cytometer. Although the immunofluorescence assay utilized the same mixed AX2 strain as the developmental assay, it is unlikely that this caused the contrasting results. Because if the uptake in wild-type cells is greater than in *Roco4 null* cells, a mixture of the two strains should still exhibit a higher uptake overall.

The weakness and strength of this project

In addition to the challenges encountered in generating CRISPR/Cas9 knockouts and GFP-inserts, this project has notable weaknesses that warrant cautious interpretation of the data presented. The developmental assay and immunofluorescence assay were conducted once, potentially introducing variability and reducing the reliability of the

results. While the flow cytometry assay was performed in duplicate, the lack of additional replicates raises concerns about the reproducibility of the findings. On top of that, due to the lack of data on which Rab proteins pT72 Rab8 binds in Dictyostelium, the results cannot confirm which specific Rab proteins are phosphorylated by Roco4. Furthermore, since the AX2 strain from the developmental and immunofluorescence assay was a mix from both AX2 and *Roco4 null* cells, the data from these assays should be interpreted with caution.

However, the obstacles of creating the CRISPR/Cas9 knockouts and GFP-inserts also serve as the strength of this project. This project is a true portrayal of science and the many hardships that come with doing research. It serves as a foundation for further development and refinement of the CRISPR/Cas9 process in Dictyostelium. Moreover, this project contributes to the validation of certain findings from previous research while also offering new insights. By hinting at the potential role of Roco4 in phagosome maturation and uptake, it expands upon existing knowledge and lays the groundwork for future investigations in this area. Thus, despite its challenges, this project represents a meaningful contribution to scientific understanding and serves as a platform for continued advancement in the field.

How to proceed

The next phase of this project would involve optimizing the transfection and selection procedure by for example increasing the number of Dictyostelium cells on the Klebsiella plates. This would enhance the likelihood of generating CRISPR/Cas99 knockouts and GFP-inserts, allowing for the confirmation of current findings through immunofluorescence and flow cytometry assays.

After the complete process of generating the CRISPR/Cas9 Dictyostelium knockouts and GFP-inserts has been optimized, it would be interesting to use different Cas9 vectors to create other types of mutations in Dictyostelium cells. For example, a dCas9 (Dox-on) vector could be helpful for the *mybW* gene since it allows control of the inhibition of the gene expression. This makes it possible to inhibit the expression of *mybW* during certain phases of the cell cycle revealing more insights into its functional role. Additionally, Cas9 nickase, which induces single-strand breaks and has fewer off-target effects than Cas9, could simplify gRNA design for the highly repetitive and AT-rich genome of Dictyostelium.

For further research into the phosphorylation of Rab proteins by Roco4 it would be interesting to determine which Dictyostelium Rab proteins pT72 Rab8 binds to. Bioinformatics could be used to identify potential binding targets by aligning amino acid sequences and predicting antigenic regions. Subsequent experimental studies, such as immunoprecipitation or Western blotting with Dictyostelium lysates, could then confirm the binding of the antibody to specific Rab proteins.

On top of that, it would be interesting to test the effect of overexpressing Roco4 on the phosphorylation of Rab proteins. Since Rab phosphorylation by LRRK2 has a short time window, it is expected that Roco4 has a similar short time window of phosphorylating

Rabs. By overexpressing Roco4 it is possible to increase the chances of observing the phosphorylation process.

Regarding phagosome maturation, the next step would be to observe how Roco4 is involved in this process. After identifying which Rab proteins are phosphorylated by Roco4 it would be interesting to knockdown those specific Rab proteins using RNA interference techniques to investigate whether Roco4 directly affects phagosome maturation or indirectly via Rab proteins. Moreover, live fluorescence imaging utilizing pHrodo could be used to examine whether Roco4 accelerates or slows down phagosome maturation.

Bibliography

Tetsuya Muramoto, 2022. Home > Gene > Plasmid Detail / NBRP Nenkin. *NBRP Nenkin.*
Machery-nagel, 2023. Bioanalysis n NucleoSpin ® Gel and PCR Clean-up PCR clean-up and Gel extraction. *Bioanalysis n NucleoSpin ® Gel and PCR Clean-up PCR clean-up and Gel extraction User Manual.*
Gaudet, P., Pilcher, K. E., Fey, P. & Chisholm, R. L., 2007. Transformation of Dictyostelium discoideum with plasmid DNA. *Nature protocols,* 6, 2(6), pp. 1317-1324.
Linkner, J. et al., 2012. Highly effective removal of floxed Blasticidin S resistance cassettes from Dictyostelium discoideum mutants by extrachromosomal expression of Cre. *European Journal of Cell Biology,* 2, 91(2), pp. 156-160.
Yamashita, K., Iriki, H., Kamimura, Y. & Muramoto, T., 2021. CRISPR Toolbox for Genome Editing in Dictyostelium. *Frontiers in Cell and Developmental Biology,* 8.Volume 9.
Muramoto, T., Iriki, H., Watanabe, J. & Kawata, T., 2019. Recent Advances in CRISPR/Cas9-Mediated Genome Editing in Dictyostelium. *Cells 2019, Vol. 8, Page 46,* 1, 8(1), p. 46.
Chu, V. T. et al., 2015. Increasing the efficiency of homology-directed repair for CRISPR-Cas9-induced precise gene editing in mammalian cells. *Nature Biotechnology 2015 33:5,* 3, 33(5), pp. 543-548.
Lin, S., Staahl, B. T., Alla, R. K. & Doudna, J. A., 2014. Enhanced homology-directed human genome engineering by controlled timing of CRISPR/Cas9 delivery. *eLife,* Volume 3, p. e04766.
Concordet, J. P. & Haeussler, M., 2018. CRISPOR: intuitive guide selection for CRISPR/Cas9 genome editing experiments and screens. *Nucleic Acids Research,* 7, 46(W1), pp. W242-W245.
Ogasawara, T. et al., 2022. CRISPR/Cas9-based genome-wide screening of Dictyostelium. *Scientific Reports,* 12, 12(1), p. 11215.
Gilsbach, B. K. et al., 2012. Roco kinase structures give insights into the mechanism of Parkinson disease-related leucine-rich-repeat kinase 2 mutations. *Proceedings of the National Academy of Sciences of the United States of America,* 6, 109(26), pp. 10322-10327.
Fasiczka, R., Naaldijk, Y., Brahmia, B. & Hilfiker, S., 2023. Insights into the cellular consequences of LRRK2-mediated Rab protein phosphorylation. *Biochemical Society Transactions,* 4, 51(2), pp. 587-595.
Thirstrup, K. et al., 2017. Selective LRRK2 kinase inhibition reduces phosphorylation of endogenous Rab10 and Rab12 in human peripheral mononuclear blood cells. *Scientific Reports 2017 7:1,* 8, 7(1), pp. 1-18.
Rupper, A., Grove, B. & Cardelli, J., 2001. Rab7 regulates phagosome maturation in Dictyostelium. *Journal of Cell Science,* 7, 114(13), pp. 2449-2460.
Bush, J. et al., 1993. Cloning and characterization of five novel Dictyostelium discoideum rab-related genes. *Gene,* 12, 136(1-2), pp. 55-60.
Buczynski, G. et al., 1997. Evidence for a recycling role for Rab7 in regulating a late step in endocytosis and in retention of lysosomal enzymes in Dictyostelium discoideum.. *Molecular Biology of the Cell,* 8(7), p. 1343.
Rupper, A. & Cardelli, J., 2001. Regulation of phagocytosis and endo-phagosomal trafficking pathways in Dictyostelium discoideum. *Biochimica et Biophysica Acta (BBA) - General Subjects,* 3, 1525(3), pp. 205-216.
Liu, Z. et al., 2016. LRRK2 autophosphorylation enhances its GTPase activity. *The FASEB Journal,* 1, 30(1), p. 336.

Lee, H. et al., 2020. Stem Cell Reports Article LRRK2 Is Recruited to Phagosomes and Co-recruits RAB8 and RAB10 in Human Pluripotent Stem Cell-Derived Macrophages.
Yeo, J. C., Wall, A. A., Luo, L. & Stow, J. L., 2016. Sequential recruitment of Rab GTPases during early stages of phagocytosis. *Cellular Logistics,* 1.6(1).
Hanadate, Y., Saito-Nakano, Y., Nakada-Tsukui, K. & Nozaki, T., 2016. Endoplasmic reticulum-resident Rab8A GTPase is involved in phagocytosis in the protozoan parasite Entamoeba histolytica. *Cellular microbiology,* 10, 18(10), pp. 1358-1373.
Steger, M. et al., 2016. Phosphoproteomics reveals that Parkinson's disease kinase LRRK2 regulates a subset of Rab GTPases. *eLife,* 1.Volume 5.
Kuwahara, T. et al., 2016. LRRK2 and RAB7L1 coordinately regulate axonal morphology and lysosome integrity in diverse cellular contexts. *Scientific reports,* 7.Volume 6.
Park, J., Bae, S. & Kim, J. S., 2015. Cas-Designer: a web-based tool for choice of CRISPR-Cas9 target sites. *Bioinformatics,* 12, 31(24), pp. 4014-4016.
Heigwer, F., Kerr, G. & Boutros, M., 2014. E-CRISP: fast CRISPR target site identification. *Nature Methods 2014 11:2,* 1, 11(2), pp. 122-123.
Haver, H. N. & Scaglione, K. M., 2021. Dictyostelium discoideum as a Model for Investigating Neurodegenerative Diseases. *Frontiers in Cellular Neuroscience,* 10, Volume 15, p. 759532.
Gilsbach, B. K., 2014. Biochemical and structural characterization of Roco4: A model to understand LRRK2 mediated parkinson´s disease.
Cheeseman, I. M. & Desai, A., 2008. Molecular architecture of the kinetochore–microtubule interface. *Nature Reviews Molecular Cell Biology 2008 9:1,* 1, 9(1), pp. 33-46.
van Egmond, W. N. & van Haastert, P. J., 2010. Characterization of the Roco protein family in Dictyostelium discoideum. *Eukaryotic Cell,* 5, 9(5), pp. 751-761.
Cookson, M. R., 2016. Cellular functions of LRRK2 implicate vesicular trafficking pathways in Parkinson's disease. *Biochemical Society Transactions,* 12, 44(6), pp. 1603-1610.
Hu, J. et al., 2023. Small-molecule LRRK2 inhibitors for PD therapy: Current achievements and future perspectives. *European Journal of Medicinal Chemistry,* 8, Volume 256, p. 115475.
Galatsis, P., Henderson, J. L., Kormos, B. L. & Hirst, W. D., 2014. Leucine-Rich Repeat Kinase 2 (LRRK2) Inhibitors. *Topics in Medicinal Chemistry,* 12, Volume 18, pp. 111-148.
Cardoso, C. M., Jordao, L. & Vieira, O. V., 2010. Rab10 Regulates Phagosome Maturation and Its Overexpression Rescues Mycobacterium-Containing Phagosomes Maturation. *Traffic,* 2, 11(2), pp. 221-235.
Vieira, O. V., Botelho, R. J. & Grinstein, S., 2002. Phagosome maturation: aging gracefully. *Biochemical Journal,* 9, 366(3), pp. 689-704.
Jinek, M. et al., 2012. A programmable dual-RNA-guided DNA endonuclease in adaptive bacterial immunity. *Science,* 8, 337(6096), pp. 816-821.
Veltman, D. M., Akar, G., Bosgraaf, L. & Van Haastert, P. J., 2009. A new set of small, extrachromosomal expression vectors for Dictyostelium discoideum. *Plasmid,* 3, 61(2), pp. 110-118.
Härtlova, A. et al., 2018. LRRK2 is a negative regulator of Mycobacterium tuberculosis phagosome maturation in macrophages. *The EMBO Journal,* 6.37(12).
Taylor, J. A., Gardner, A., Carlson, J. & Westbrook, A. L., 2006. *The BSCS 5E Instructional Model: Origins, Effectiveness, and Applications,* s.l.: s.n.
Eichinger, L. et al., 2005. *The genome of the social amoeba Dictyostelium discoideum,* s.l.: s.n.
Sekine, R., Kawata, T. & Muramoto, T., 2018. CRISPR/Cas9 mediated targeting of multiple genes in Dictyostelium. *Scientific Reports 2018 8:1,* 5, 8(1), pp. 1-11.

Yamashita, K., Iriki, H., Kamimura, Y. & Muramoto, T., 2021. CRISPR Toolbox for Genome Editing in Dictyostelium. *Frontiers in Cell and Developmental Biology,* 8.Volume 9.
Gilsbach, B. K. et al., 2012. Roco kinase structures give insights into the mechanism of Parkinson disease-related leucine-rich-repeat kinase 2 mutations. *Proceedings of the National Academy of Sciences of the United States of America,* 6, 109(26), pp. 10322-10327.
Steger, M. et al., 2016. Phosphoproteomics reveals that Parkinson's disease kinase LRRK2 regulates a subset of Rab GTPases. *eLife,* 1.5(JANUARY2016).
van Egmond, W. N. & van Haastert, P. J., 2010. Characterization of the Roco protein family in Dictyostelium discoideum. *Eukaryotic Cell,* 5, 9(5), pp. 751-761.
Iriki, H., Kawata, T. & Muramoto, T., 2019. Generation of deletions and precise point mutations in Dictyostelium discoideum using the CRISPR nickase. *PLoS ONE,* 10.14(10).
Kortholt, A., Gilsbach, B. & van Haastert, P., 2012. Dictyostelium discoideum: A Model System to Study LRRK2-Mediated Parkinson Disease. Mechanisms in Parkinson's Disease - Models and Treatments.. *InTech. ,* Volume 07.
Liou, A. K., Leak, R. K., Li, L. & Zigmond, M. J., 2008. Wild-type LRRK2 but not its mutant attenuates stress-induced cell death via ERK pathway. *Neurobiology of disease,* Issue 32, pp. 116-124.
Carballo-Carbajal, I. W.-E. S. R. G. C. et al., 2010. Leucine-rich repeat kinase 2 induces α-synuclein expression via the extracellular signal-regulated kinase pathway.. *Cellular signalling,* Issue 22, pp. 821-827.
Chen, C. et al., 2012. LRRK2 activates MKK4- JNK pathway and causes degeneration of SN dopaminergic neurons in a transgenic mouse model of PD. *Cell Death Differ,* Issue 19, pp. 1623-1643.
Maekawa, T. et al., 2016. Leucine-rich repeat kinase 2 (LRRK2) regulates α-synuclein clearance in microglia.. *BMC Neurosci,* Issue 17.
Rui, Q. et al., 2018. The Role of LRRK2 in Neurodegeneration of Parkinson Disease.. *Curr. Neuropharm,* Issue 16, pp. 1348-1357.
Hatano, T. et al., 2007. Leucine-rich repeat kinase 2 associates with lipid rafts. *Hum. Mol Genet,* Issue 16, pp. 678-690.
Alegre-Abarrategui, J. et al., 2009. LRRK2 regulates autophagic activity and localizes to specific membrane microdomains in a novel human genomic reporter cellular model. *Hum. Mol. Genet,* Issue 18, pp. 4022-4034.
Biskup, S. et al., 2006. Localization of LRRK2 to membranous and vesicular structures in mammalian brain. *Neurol,* Issue 60, pp. 557-569.
Galter, D. et al., 2006. LRRK2 expression linked to dopamine-innervated areas. *Neurol,* Issue 59, pp. 714-719.
Higashi, S. et al., 2007. Localization of Parkinson's disease-associated LRRK2 in normal and pathological human brain.. *Brain Res,* Issue 1155, pp. 208-219.
Rosenbusch, K. E., Fikse, L., Aresti, J. & Kortholt, A., 2021. Chapter 4 Rab family members are conserved Roco substrates.
Fei, D. et al., 2008. Regulation of contractile vacuole formation and activity in Dictyostelium. *The EMBO Journal,* Issue 27, pp. 2064 - 2076 .
Yeo, J. C., Wall, A., Luo, L. & tow, J. L., 2016. Sequential recruitment of Rab GTPases during early stages of phagocytosis. *Cellular Logistics,* Issue 6.
Machery-Nagel, 2023. Bioanalysis n NucleoSpin ® Plasmid EasyPure Plasmid DNA purification.
Jeong, G. R. & Lee, B. D., 2020. Pathological functions of LRRK2 in Parkinson's disease. *Cells,* Issue 9, p. 2565.

Acknowledgements

I'd like to thank the entire cell biochemistry department for creating such a positive and welcoming environment during my internship. While I'm not the most talkative person in groups, I truly appreciated being included in every group lunch and the willingness of everyone to help with my research. On top of that I'd like to thank Arjan for consistently guiding us through this project. Whenever Gargi, Eelco, and I were stuck or needed help interpreting something, Arjan was always there to assist. Most of all, I would like to thank Eelco and Gargi for their help, feedback, patience, and positive attitude during this project. As someone who already knew that research wasn't for him, I feared having trouble pushing myself through another research project. But the two of you created a very flexible, positive, challenging, and fun learning environment that guided me through this project without it ever feeling like a burden. Eelco, thanks for always making me think for a little bit longer when I rushed in with questions and pushing me in the right direction instead of feeding me the answers. This allowed me to gain confidence in my own ideas and made it very welcoming for me to come with my own suggestions of what to do next. Gargi, thanks for all the extra labwork you did to help me, such as preparing cells for my experiments, finishing my experiments when I had to leave for volleyball practice, culturing my cells through the weekend and so much more hahaha. On top of that, thanks for occasionally laughing with me about the state of my project. Joking together about all the transformants failing or another unexplainable contamination made these types of situations much lighter and easier to handle. I'm very happy that my (most likely) last lab experience was as a part of this research group and under both of your supervision so that this part of my education can come to a very positive end. Thank you so much.

Appendences:

Supplementary table 1:

Primer	Sequence	Annealing Temperature
Guide RNA's		
ROCO4		
FW-gRNA-ROCO4-60	AGCACAACAACAATATACTAGGGT	NA
REV-gRNA-ROCO4-60	AAACACCCTAGTATATTGTTGTTG	NA
FW-gRNA-ROCO4-55	AGCAAACTACAACAACAATATACT	NA
REV-gRNA-ROCO4-55	AAACAGTATATTGTTGTTGTAGTT	NA
FW-gRNA-ROCO4-56	AGCAACTACAACAACAATATACTA	NA
REV-gRNA-ROCO4-56	AAACTAGTATATTGTTGTTGTAGT	NA
MybW		
FW-gRNA-MybW_N	AGCAAGATTTATTCTCTTTAGCAT	NA
REV-gRNA-MybW_N	AAACATGCTAAAGAGAATAAATCT	NA
GFP primers		
ROCO4		
HR5-GFP-ROCO4	ATCAGTAACATTAAAAAAGAAAGGTT AAAAAAAAAAAAAAAAAAAAATAATAA AAAAAAAATAAATAAATAAAAAAATG ATGTCAAAAGGTGAAGAATTATTTAC AG	60
3'HR-GFP-ROCO4-new	TATTATTAAATCTTTCATTGGACCAAT AACATCAATACCTACTCGTGTGTAATG TTGATGTAGTTGTTGGGATTCTTGTA ATTGTTGTGATGAATCTTTGGATCTAC TACCTCCTGAACC	60
MybW		
HR5-GFP-MybW	TTTATTTTATATTTTTATATATTAAAGT TACAATAATATAGATAATAATAATAAT AATAATAATAATAATAATAATTATAAT AATTATAGAAATGTCAAAAGGTGAA GAATTATTTACAG	60
HR3-GFP-MybW	CCCTCCAAATTATTAATATTATTATAAT GTGTTTTCAAGTATAAATGCTTACGTT CTAATGCTAAAGAGAATAAATCTTGT TCTGCTTTGGATCTACTACCTCCTGAA CC	60
Blast primers		
ID		
HR5-ACT6-ROCO4	TAATAAAAAAAAAATAAATAAATAAA AAAATGGATTCATCACAACAATTACAA GAATCCCAACAACTACTTTTTAAATAA AAAATGGGTTTTTTTTAAGTAAAG	62
HR3-mhcA-ROCO4	CTTAAATGTTGTATCTAAACTATTCAT TACTGATATTATTAAATCTTTCATTGG ACCAATAACCATTTTATTTAATATACTA AATAATAAAAAAGTTAAAAAATGATC	62
MybW		
HR5-ACT6-MybW	CATTTCTTTAATTTCCACAATTTACACA AATTATATTTATTTTATATTTTTATATA TTAAAGTTACTTTTTAAATAAAAAATG GGTTTTTTTTAAGTAAAG	62
HR3-mhcA-MybW	GCTTGTTCTTTTTGAATTTGATAAAAT GGTAAGTATGTTCGATAAAGAAGAG ATTTTTGTAATATATTCATTCCCCATTT TATTTAATATACTAAATAATAAAAAAG TTAAAAAATGATC	62

Supplementary table 1 list of Primers used throughout the project.

Supplementary table 2:

Colony PCR/Sequence primers		
tracr_RV_screen	AAGCTTAAAAAAAGCACCGACTCGGTGCC	
NeoUp_seq	TCCTGCAGTTCATTCAGGGC	
Genome PCR/Sequence primers		
ROCO4		
ROCO4_FW_genome	GAATGGGAAAATAGAGTGTGTTTGG	62
ROCO4_RV_genome	CTGCTTCCTCGTCAGCATC	60.2
ROCO4_FW_seq	AAATATATATATATAATATCAGTAACATTAAAAAAGAAAGG	59.5
ROCO4_RV_seq	CATCTGTATCAAAATATACTATACGATAGGTTTC	60.7
MybW		
MYBW_FW_genome	GACACCCATCTTATCTCAGAATCC	60.7
MYBW_RV_genome	GTAAGTATGTTCGATAAAGAAGAGATTTTTG	60.8
GFP_FW	CAGAAGTTAAATTTGAAGGTGATACATTAG	60.5
GFP_RV	CTAATGTATCACCTTCAAATTTAACTTCTG	60.6

Supplementary table 2 second list of Primers used throughout the project.

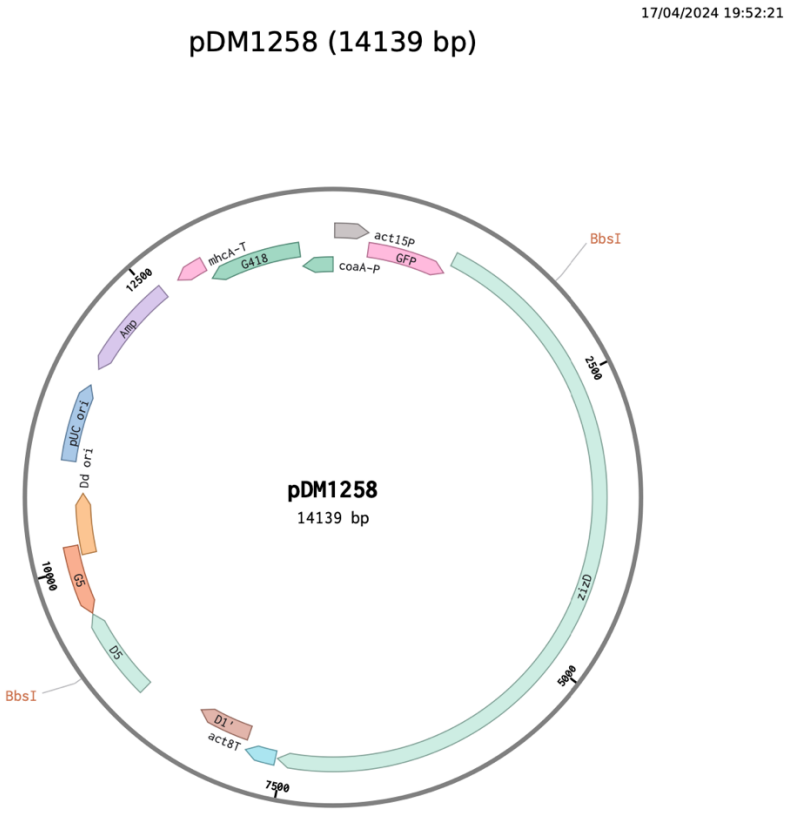

supplementary figure 1 pdm1258 plasmid map, used to amplify GFP sequence.

17/04/2024 19:57:23

pDM326 (6431 bp)

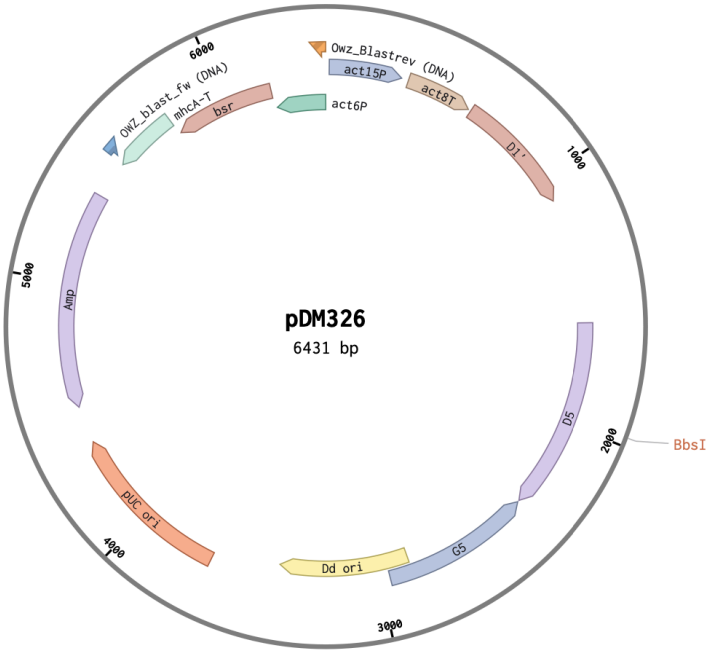

supplementary figure 2 pdm325 plasmid, used to amplify blast sequence.

Protocols:

Immunofluorescence for Dictyostelium AX2 and ROCO4 null with mammalian Rab8A(PT72) antibody protocol.

1. Seed 0.8 X 10^5 cells in polyl lysine coated IBIDI®chamber.
2. Incubate at 21 ˚C overnight in HL-5 media.
3. Add 4uL of Texas red zymosan beads to 800uL of media. (5 beads/cell) Vortex and spin down shortly.
4. Sonicate (Duty cycle: 70%, output control: 6) the media with Zymosan beads using a BRANSON® SONIFIER 450.
5. Aspirate the media out of the IBIDI chambers with a pipette.
6. Add 200 uL of the HL-5 media + zymosan mixture to the IBIDI chambers.
7. Incubate with the zymosan for one and a half hour at 21oC.
8. Aspirate the liquid using a pipette.
9. Wash the wells with PB twice. (This step removes the medium and excess zymosan)
10. Add 200uL Fixation buffer (4%PFA in PB,) and incubate for 15 mins.
11. Wash 3 times with PB.
12. Add 200uL Permeabilization buffer (0.2-0.4% Triton-X in PB), incubate for 15-20mins.
13. Wash 3 times with PB.
14. Add 200uL Blocking buffer and incubate for 1 hour.
15. Remove the blocking buffer (No washes needed).
16. Add primary antibody Rab8A (Pt72) (1:500) in blocking buffer (3% BSA 0.1% Tween in PB), incubate overnight.
17. Wash 5 times with washing buffer
18. Add secondary antibody (1:400) (α-Donkey-anti-rabbit-green fluorophore)
19. Wash with wash buffer. (0.1% Triton in PB).
20. Take it to the microscope.

Flow cytometry:

1. Seed 0.5 x 10^5 cells in a flat-bottom 96-well plate.
2. Incubate in HL-5 media at 21 ˚C overnight.
3. Add 5 beads/cell Fitc and/or pHrodo to media and vortex and spin down shortly.
4. Push this through a needle to get rid of zymosan clumps.
5. Incubate at 21oC for 1.5 hours.
6. Wash with ice-cold PB.
7. Transfer cells to a conical bottom 96-well plate.
8. Centrifuge at 300 RCF, 21 ˚C for 3 minutes and wash with PB. Repeat this thrice.
9. Measure using a flow cytometer.